POLITECNICO DI TORINO

Master of Science in Biomedical Engineering

Master's Thesis

Implementing novel techniques for cellular labeling and optical recording in multiple brain regions in behaving mice

Supervisors

Prof. Candido Pirri

Prof. John Assad

Candidate

Giulia Micelli

December 2018

Ai miei nonni

Angelo e Pietro

Abstract

Different brain regions give a unique contribution in the control of movements. It has been demonstrated that some circuit functions are altered in movement disorders. It would be interesting to analyze the mechanism by which the flow of information passes through basal ganglia nuclei, whose functions are alterated in presence of desease like Parkinson, in the initiation of a movement studying the neural activity in different regions simultaneously. In this work, the role of striatum for the direct pathway (D1) was investigated in behaving mice using an optical fiber photometry system to measure calcium signal which is a measurement of neural activity. The goal is to understand if, what happens when mice decide to initiate an action and get ready to perform it, is crucially explained by the activity of specific neurons. Mice were trained to initiate spontaneous movements using a self-timed behavior paradigm. AAV virus encoding GCaMP6f as the calcium protein indicator has been used to label only neurons belonging to the direct pathway in transgenic animals. The experiment was conducted with two optical fibers implanted bilaterally in the dorsal striatum of two genetically modified D1-cre mice. Additional, this experiment was exactly repeated but using novel silk-coated tapered optical fibers to overcome limits coming from injection procedure and the cut fiber geometry. The signal dF/F, representing the change in fluorescence over the baseline of a given period, has been used to compare neural activity recorded with the two different optical fibers. Signal recorded in animals with standard optical fibers contains ramps

supposed to be related to the movement timing with a similar trend and amplitudes in both mice. An accelerometer has been used during the recording session to obtain mouse's position revealing that ramps in activation of direct-pathway neurons are not related to the ongoing movements of the animal while it's preparing to move. Changes in fluorescence obtained with the novel optical fibers from three different mice contain only noise and not information about the calcium flux. Histological images from one mouse confirm a very low expression of the fluorescent molecule in the striatum. The next step, to analyze simultaneously neural activity at different depths in the striatum, is using an innovative system of mirrors to change the input light angle in the tapered fiber once D1-type neurons are labeled with the GCaMP indicator.

Contents

List of Figures

Chapter 1

Introduction

Different brain regions give a unique contribution in the control of movements. It has been demonstrated that some circuit functions are altered in movement disorders. For example, Parkinson's disease alters the function of the basal ganglia circuit resulting in reduced ability to control movement. It would be interesting to analyze the mechanism by which the flow of information passes through basal ganglia nuclei in the initiation of a movement studying the neural activity in different regions simultaneously. Electrophysiology techniques allow the recording of electrical activity from a big population of neurons with a spatial resolution of a single neuron and a temporal resolution of milliseconds. On the other hand, these techniques have very low neuronal selectivity because they act on an anatomical area of the brain that includes a complex system of different cell types. The development of genetic manipulations and the creation of transgenic animals has been of great help in recent years. In fact, with the development of genetically encoded fluorescence-based indicators and optical devices, recording from a bigger, genetically-labeled population of neurons is possible with a small implant in the brain. Optical fibers are devices that allow to record bulk population neural activity using calcium protein indicators. This method, even if it doesn't have a single-cell resolution, requires only the implantation of such tiny devices above the region of interest with minim

tissue damage. Standard optical fibers emit and collect light from their flat end. To illuminate most distant neurons (beyond 100 μm of radius) more power is required due to tissue attenuation and this may cause other disadvantages such as increased photobleaching, which limits the time of recording sessions. A solution to this problem could be the use of different fibers that, by varying the geometry, overcome the limitations of standard cut fibers. Tapered fibers allow recording of the neural activity from a bigger population because they emit light also along their length and can be implanted inside the region of interest, overcoming the tissue attenuation issue. The tissue damage due to the invasive brain perturbation for their implantation is limited with the tapered geometry because they are thiner than the standard fibers. These fibers have a better spatial resolution, in fact they allow the recording from neurons at different positions in the brain simultaneously because, just by varying the input light angle, they can illuminate small regions from localized sites along their length [9] .

Isolating activity from specific populations is possible by labeling them with fluorescent proteins, whose brightness is proportional to ambient calcium. Virus encoding the protein with a cell-type specific promoter and/or cre-dependece is injected into an area of the brain through a small hole in the skull. This results in the brain being perturbed twice because fiber insertion follows the injection step, implying higher risk of tissue damage and probability that the injection and implantation will not be aligned. A way to increase the chances of success and make surgery easier is to reduce the two steps to one. The fiber can be coated with a polymer solution in which the virus is dissolved. The polymer degrades after implantation, thereby releasing the virus and allowing uniform protein expression over the entire length of the fiber in the cell type of interest [11].

Basal ganglia circuit is a structure in the brain that seems to have a role in movement initiation. The main inputs to this circuit, from cerebral cortex and thalamus, synapse in the striatum, which contains the so-colled striatal projection

neurons (SPNs) with two primary phenotypes: D1-type SPNs of the direct pathway and D2-type SPNs of the indirect pathway. The direct pathway is hypothesized to provide positive feedback to the cortex and so to facilitate movements, while the indirect pathway is hypothesized to inhibit movements.

In this work, the role of striatum for the direct pathway (D1) was investigated using an optical fiber photometry system to measure calcium signal, which is a measurement of neural activity. The experiment was conducted with two optical fibers implanted bilaterally in the dorsal striatum of two genetically modified D1-cre mice. AAV virus, encoding GCaMP6f as the calcium protein indicator and injected in the dorsal striatum, labeled only neurons belonging to the direct pathway. Additional, this experiment was exactly repeated but using silk-tapered fibers to overcome limits coming from injection procedure and the cut fiber geometry. To study the role of direct-pathway neurons in the control of movements, the goal is to analyze neural activity related to a stereotyped, spontaneous movement; the idea is to understand if, what happens when mice decide to take an action and get ready to perform it, is crucially explained by the activity of specific neurons. A self-timed behavior paradigm was chosen and mice were trained to move after an arbitrary time interval from a cue stimulus so that the action is spontaneous and not an instantaneous reaction to the stimulus.

Chapter 2

State of the art

In this work the attention was focused on the role of D1-type neurons of the striatum. In general, neural acitivity can be measured *in vivo* with two families of techniques, electrophysiology or visualization of fluorescent proteins. Both techniques aim to understand the relationship between the activity of neurons and behavior.

2.1 Striatum and D1-type Neurons

The basal ganglia (BG) and related nuclei consist of a variety of subcortical cell groups involved in control voluntary actions. This circuit is alterated in presence of diseases that involve movement disorders. [6]

The BG are composed of four main nuclei: striatum, internal and external globus pallidus (GPi and GPe), subthalamic nucleus, substantia nigra (reticular pars - SNr and compact pars -SNc) .

Internal globus pallidus (GPi) and Substantia nigra reticulata (SNr) are the output of the circuit. Striatum is the initial input center of the basal ganglia (BG) system.

The striatum receives input from the cortex and from the thalamus and, when it is excited by the signal coming from the motor cortex, we can see two different

pathways because the striatum has two major different neuron types.

Most of neurons (95%) in the striatum are named GABAergic striatal projection neurons (SPNs), also known as Medium spiny neurons (MSNs); they have two primary phenotypes (characteristic types): D1-type MSNs of the direct pathway, also known as dSPNs, and D2-type MSNs of the indirect pathway, also known as iSPNs. Most of SPNs contain only D1-type or D2-type dopamine receptors, but a tiny subpopulation of them exhibit both phenotypes.

Direct-pathway striatonigral neurons (dSPNs) expressing D1 receptors project to the substantia nigra. Although these neurons are inhibitory, the pathway overall is excitatory and provides a positive feedback to cortex Figure 2.1. Neurons from the cortex to the striatum are excitatory (+). When the signal arrives to these neurons, they are activated. Between striatum and globus pallidus internal (GPi) neurons are inhibitory (-) and GPi is active at rest. So, when the striatum neurons are activated, they inhibit the activity of GPi. The GPi at rest keeps the thalamus inhibited and neurons from GPi to thalamus are inhibitory. When the signal arrives, the thalamus is activated and a positive feedback is sent to the cortex.

Indirect-pathway striatopallidal neurons (iSPNs) expressing D2 and A2A receptors project to the external segment of the globus pallidus Figure 2.1. D2 iSPNs inhibit the GPe through the the inhibitoty connections between the two. The inhibitory connections between GPe and subthalamic nucleus activate the subthalamic nucleus which, in turn, activate GPi (excitatory connections). The GPi inhibits the thalamus, decreasing its activity, so overall there is a negative feedback to the cortex when iSPNs are active.

Thalamus drives the cortex, but GPi inhibits thalamus, so there is likely a kind of balance between direct and indirect pathway in regulating cortical firing. In fact, the two pathways have opposing effects on movement: activity of dSPNs is supposed to facilitate movement, whereas activity of indirect pathway iSPNs is hypothesized to inhibit movement [6].

Who modulates the balance between direct and indirect pathway? DA, released by the neurons of the substantia nigra pars compacta (SNc), may govern this balance between indirect and direct pathways. If you lose the DA projection, you get Parkinson desease, which results in decreased motor output (rigidity, slow movements), as if balance favors the indirect pathway.

Here, the role of the striatum for the direct pathway (D1) has been investigated in a simple task in which mice learn to lick for a juice reward in response to a light stimulus.

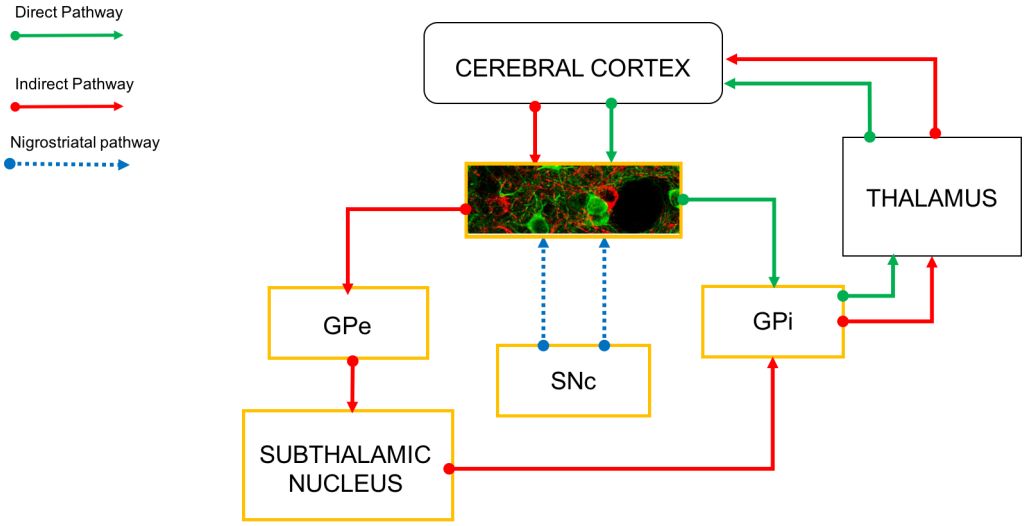

Figure 2.1: D1 and D2 pathway

2.2 Electrophysiology

Electrophysiology techniques measure electrical activity of neurons while they communicate with each other using electrical and chemical signals [1]. Three main categories of electrophysiology can be distinguished according to the position of the recording instruments (electrodes) in relation to the cells.

Extracellular recording is the easiest and simplest way to record from neurons with a minimal invasiviness. This technique positions an electrode outside the neuron of interest and then there is a ground electrode that allows the electrode to measure the potential between the two probes, which changes as the neuron fires. For *in vivo* applications, electrodes can be inserted in the brains of live animals (Figure 2.2). When there is not neural activity, the difference in potential between the electrodes is equal to zero. Neurons communicate via electrical signals called action potentials, which transmit information from the sensing-part of the neuron (dendrites plus cell body) to the information-relaying part of the neuron (axon terminals) where the signal is transmitted to downstream neurons via release of chemical messengers called neurotransmitters. When an action potential is present, and so the neuron's membrane depolarizes, a flux of positive charge enters the cell, causing a decrease in positive ions around the recording electrode, thus the electrode senses a decrease in voltage. Then, once the action potential passes, positive charge exits the cell, resulting in repolarization and return of the measured extracellular potential to baseline.

An important limitation in using an electrode to record the neural activity is that it could be tough to define if the activity recorded is generated by one neuron or a bunch of neurons around the electrode tip. The use of multiple electrodes can overcome this limit and allows recording multiple cells at once. Examples of multi-electrodes are tetrodes, four small electrodes wrapped togheter, or Ăň multielectrode arrays (MEA), grids of electrodes grouped in a single device. It is important to study the activity of multiple neurons at a time since it allows to study connectivity and timing within different neurons. The signal recorded with each individual microelectrode can be easily compared and single cell signals can be obtained by recording from multi electrodes. Each neuron recorded has its specific and reproducibile waveform that most of the time can be obtained processing the signal with a triangulation

method based on the position of the electrodes and characteristic shape of a recording. Signal recorded in this case isn't specific for genetically-encoded cell types.

Intracellular recording requires the implant of a microelectrode into the interior of the cell to measure the potential difference between the tip of that electrode and a reference electrode positioned outside the cell. When there is an electrical voltage change across the membrane of the neuron due to synaptic events, the potential difference initially inceases and then returns to baseline ($\sim$ -70 mV). Most electrodes are a glass micropipette (<1 mm tip). These pipettes are filled with intracellular fluid solution (similar to the fluid in the cell). A silver chloride wire inside the pipette connects this solution to an amplifier that can record and process this signal[12]. When compared with an extracellular electrode, the intracellular one has the advantage of measuring potential differences in units of millivolts instead of microvolts. Moreover, with intracellular electrodes it's clearer what activity belongs to each neuron. On the other side, usign intracellular electrode is harder and only one neuron's acitivity can be recorded at a time with single electrode.

Patch clamp techniques are used to study ionic currents in individual isolated patches of cell membrane, removing the need to impale the cell. The patch-clamp microelectrode is a glass micropipette with a relatively large tip diameter tightly placed on a small area (patch) of the neuronal membrane. A suction applied through the microelectriode ensures a tight seal between pipette and membrane, which draws a part of the membrane into the tip. When a single ion channel opens in the patched membrane, all the ions must flow into the pipette and the electrical current can be measured. This configuration is called "cell-attached" mode and allows single ion channels to be recorded without changing their properties and leaving the cell intact. The patch can break leaving the electrode in contact with the whole-cell if more suction is applied. This mode, known as "whole-cell" mode, enables stable

intracellular recordings.

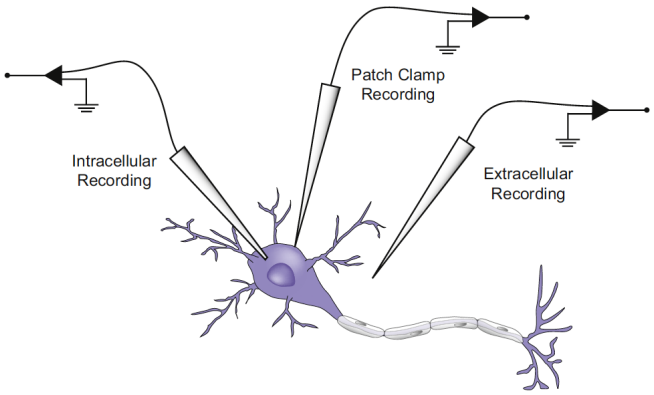

Figure 2.2: Electrophysiology techniques [1]

2.2.1 *In vivo* recordings

The best way to relate neural activity to a behavior is an *in vivo* context, letting the animal perform a behavioral task. For this reason is important to perform chronic recordings, which permit recording of neural activity over days. Fiber optic cannulae or electrodes are implanted into the brain with a surgery operation. *In vivo* recording most of the time is an extracellular one, performed with electrodes, tetrode or multielectrode arrays. Placing an electrode for intracellular or patch clamp recording is harder but still possible with special equipment. A sharp pipette can be used to impale cells for sharp electrodes recordings. Two-photon microscopy can be used with an animal expressing a fluorescent protein in a cell type to visualize the patch pipette on the surface of the membrane. In conclusion, it is usually preferable to study the neural activity in awake animals using the extracellular recording technique. A single electrode is usually inserted through a microdrive mounted on the surface of the brain. The microdrive allows to raise or lower the electrode to specific depths. The size and the mass of array in a microelectrode array do not allow insertion into deep brain structures, but only placement on the outside surface

of the brain (Figure 2.3). Conversely, tetrodes are narrow and can be inserted into relatively deep brain structures. The big adavantage is that this technique allows recording simultanously from a population of neurons obtaining a good quality signal. The single neural units can be separeted thanks to the traingulation method, and the chronic implant allows recording signals over multiple days. But if on the one hand we can distinguish the activity of different neurons, we still do not know who these neurons are because the tetrodes just collect voltage waveforms but can not identify the genetic identity of the cell that makes the waveforms. It's important to know which neurons are active at a specific time in order to make hypothesis about different brain regions involved during a behavioral tasks.

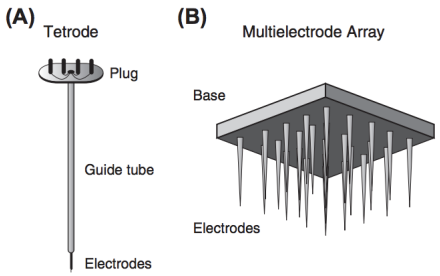

Figure 2.3: (A) Tetrode: four microwires in a guide tube. (B) Microelectrode array with 25 or more electrodes [1].

2.3 Visualization of fluorescent proteins and Calcium Imaging

Electrophysiology allows recording of neural activity with a spatial resolution of a single neuron and a temporal resolution of milliseconds. The use of multiple electrodes is necessary to record from a bigger population of neurons. However, the number of electrodes is limited by the finite space between them and the increase of risk of disruptiung circuitry and blood vessels. These techniques act on an anatomical area of the brain that includes a complex system of different cell types

and so they have a very low neuronal selectivity. The development of genetically encoded fluorescence-based indicators of neural activity and of optical devices able to read these fluorescence signals [7], involves an increase of the number of simultaneously recorded neurons genetically defined while mapping them to visualize their spatial relationships. These methods have spatial resolution from single-neuron to thousands of neurons and the temporal resolution from milliseconds to seconds, depending on the technique used.

Changes in interacellular or transmembrane calcium concentration are an important indicator of the electrical activity of neurons. Genetically encoded calcium indicators (GECIs) take advantage of the conformational changes that occur in some proteins when they bind to calcium wich alters the brightness of the indicator's fluorescence.
The first GECI constructs had a signal-to-noise ratio useful to monitor a bunch of action potentials, but not single spikes [7], while modern variants are faster and more stable allowing recondings with a resolution of single action potentials.

Fluorescence microscopes allow us to analyze specimens targeted with specific fluorophores; there are two main types of microscopes, the one-photon and the two-photon microscopes. Since the goal is to study cells activations when the animals behave in a specific way, an innovative aspect is the sufficient miniaturization of these microscopes so that they can observe neural activity in mice.

2.3.1 Head-Mounted One-Photon Microscopy

Head-Mounted micoscopes, an example of which is shown in Figure 2.4, are miniaturized devices, small enough to be mounted on the head of animal just before the imaging session; both the source for excitation light and a sensor for collecting the emitted light are in the same device. To reach deeper brain regions, GRIN lenses are chronically implanted. A cable is used for the transmission of data to an

acquisition system with a computer interface so they can be visualized and storaged. The calcium signal recorded allows spatial resolution of single neurons [2].

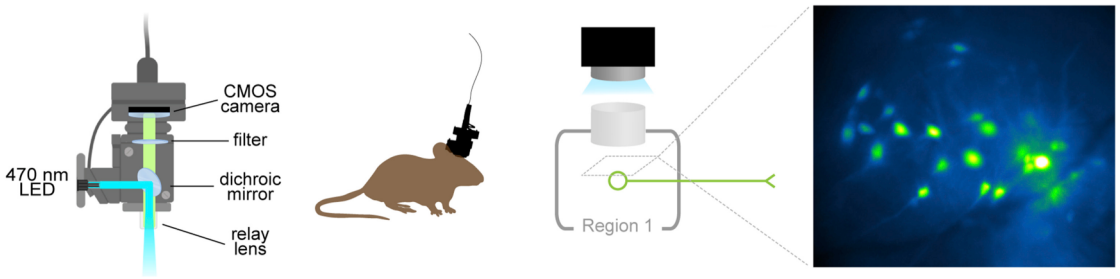

Figure 2.4: Miniaturized microscopes contain both excitation source and sensor for the emitted light. They allow recording calcium signal with a spatial resolution of a single neuron [2].

.

Figure 2.5a shows a version of a miniature one-photon microsope used to acquire images during animal behavior with a speed up to 100 Hz. Only three small gradient refractive index (GRIN) lenses are mounted directly on the mouse (1.1 g); most of the hardware is on a tabletop. The stationary setup includes an illumination source and detector, filters and a dichroic mirror. The output light of a mercury lamp, after reflecting off a dichroic mirror, is delivered to the fiber bundle through a multi-mode optical fiber. The bundle carries light to the microscope on the mouse and trasfers the fluorescence image onto a high-speed camera (EM-CCD: electron-multiplying charge-coupled device). The bundle rotates as the mouse moves thanks to the presence of a commutator.

In this microscope, the lateral resolution is limited between 2.8 and 3.9 μm and the field of view ranges from 240 to 370 μm. These limits derive from a confined packing density and a finite number of fibers that the fiber bundle can hold. Moreover, the light collection is inefficient because the space between the fibers within the bundle is finite and the illumination is time-varying. The signal-to-noise ratio (SNR) is limited and the session of recording can not go over 15 min. Penetration depths reached with

this one-photon microscopy are inferior to those achieved by two-photon imaging [3].

A variation of the microscope described above is presented in Figure 2.5b. The light source is a blue LED (light-emitting diode), whose emission is collected with a drum lens and then passed throug an excitation filter, deflected off a dichroic mirror and focused onto the sample with a gradient refractive index (GRIN) objective lens. The fluorescence is emitted back onto a CMOS sensor through the objective, the dichroic, the emission filter and an achromatic doublet lens.

This microscope, with a lateral resolution of 2.5 μm, can reach field of view up to 800 μm. Even if all these parts are mounted on the mouse's head, the total weight is of 1.9 g in 2.4 cm^3.

Images of individual neurons from freely behaving mice are obtained with a frame rate up to 100 Hz, an improvement of the signal collection and an imaging duration of ∼45 min.

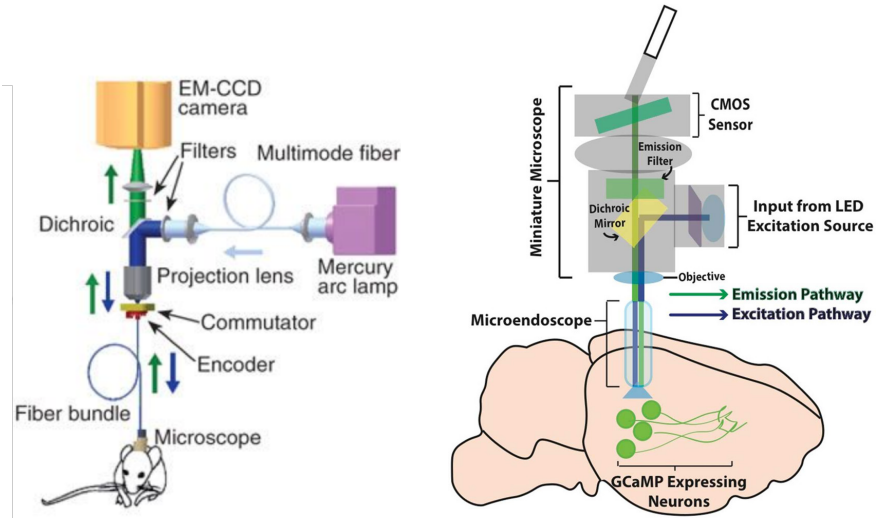

(a) **(b)**

Figure 2.5: **a** : One-photon microscopy setup [3]. **b** :One-photon microscopy setup [4]

Both these devices allow optical recording at high frame rates with a large field of view. Compared with the two-photon microscopes, they reduce a lot movement

artefacts thanks to the absence of mechanical scanning and optical sectioning. Although they may be a solution to some two-photon microscopy issues, there are some limitations to take into account. GRIN lenses suffer from optical distortions at their edges, limiting the imaging acquisition in regions on the surface, and their implant usually has diameter between 0.5 and 1 mm, causing tissue damage. Data requires post-processing to decrease crosstalk and to distribute the signal to each cellular structure because the fluorescence excitation is not limited to the focal region. Calcium signal recorded also from neurons around the focal plane creates background brightness and poor axial resolution. Moreover, in one-photon microscopy, the background fluorescence is not negligible as well as the light scattering. The single photon used as excitation has wavelengths between 390 and 700 nm; but, once out of the LED, the electron will release a photon with less energy than the excitation one since they return to its stable state.

2.3.2 Head-Mounted Two-Photon Microscopy

Two-photon microscopy is a calcium imaging technique where fluorophores absorb simultaneoulsy two photons instead of one. Two photons, having a lower energy and higher wavelength than the one used in one-photon technique, are used to obtain the same electronic transition in the molecule [13]. Using longer wavelengths (typically in the near-infrared spectrum, insted of in the UV-spectrum), allows light to reach greater depths (from 500 μm to 1 mm into tissue) but one photon in the infrared spectrum doesn't have enough energy to cause fluorescence. Two simultaneous photons, however,can converge, with a resultant molecular excitation only at the center of laser focal point, with minim tissue damage and limited scattering effects (light with longer wavelengths is less susceptible to the scattering phenomenon). This permits superior resolution because the fluorescence excitation is restricted to a narrow spot. An ultrafast infrared laser delivers light to the object. The x-y

scanner permits the laser to move across the sample, and so all the excitation is concentrated on only one small spot at a time. With the x-y position from the scanner and the light emitted, a PMT is able to construct an image with high resolution and contrast with minimal photobleaching, which allows longer recording sessions (Figure 2.6) [2].

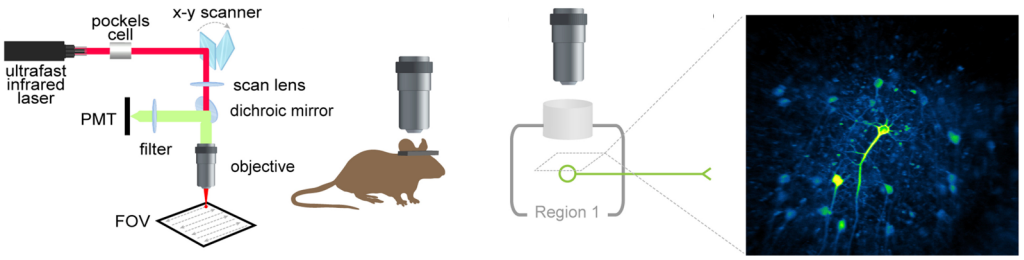

Figure 2.6: Two-photon microscope design. It can be mounted on the mouse's head allowing high resolution and contrast imaging. GRIN lenses crhonically implanted permits deeper regions in the brain to be reached. [2].

The first miniaturized two-photon microscope, weighting 25 g and long 7.5 cm, was so small and light-weight that could be carried by an adult rat[5]. In this design, a single-mode optical fiber (2 m long), used as flexible tether to connect the excitation laser and the optical setup, is the key-element for both delivery of laser pulses for the excitation and scanning of the illumination spot. Scanning the focal spot across the neural area is achieved with a piezoelectric element to excite fiber tip vibrations. The microscope mounted above a cranial window contains also excitation and barrier filters, a dichroic mirror, lenses and a photomultiplier tube (PMT), which measures and assignes the fluorescence intensities to the corresponding pixels to produce an image.

This device, because of its light weight, allows calcium transients to be measured in behaving rats, but it's too heavy to be carried by mice. The laser beam scanning across the sample makes this microscope very sensitive to quick head movements

causing motion artefacts and limiting the animal behavior. The optical sectioning implemented with two-photon microscope allows depth penetration up to $\sim 250\mu$m.

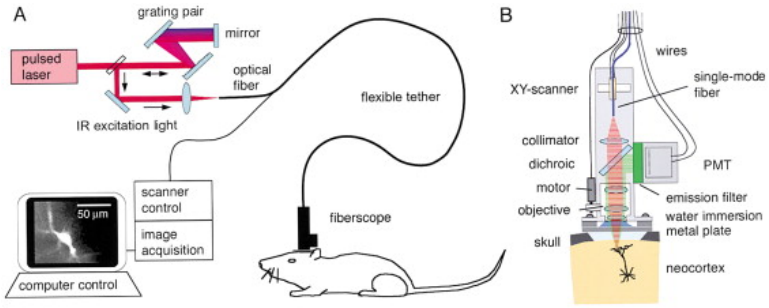

Figure 2.7: Two-photon microscopy setup [5]. A: Optical fiber tether connects the excitation laser and the optical setup. B: Microscope design.

.

Despite the advantages of two-photon calcium imaging, there are drawbacks that are limiting for neural activity recording in behaving mice. First of all, the size of different parts are big enough to prevent some natural behavior and are too heavy to be carried by mice. Further, the laser scanning across the sample requires a small field of view for reasonable temporal resolution. Then, the all setup requires very expensive components that can range from half a million-dollars to two-million dollars.

2.3.3 Fiber Photometry

Fiber photometry, a technique in the calcium imaging family, uses chronically implanted optical fibers to record bulk population neural activity in freely moving mice. Optical fibers are used to transport the exciting light, with appropriate wavelength, from LEDs to GECI; then, fluorescence emitted back is collected with the same fiber and sent to a photoreceiver. Dichroic mirrors are used to divide excitation and emission light [2] (Figure 2.8). Fiber photometry is easy to implement and requires a cheaper setup compared with other optical techniques.

An example of fiber photometry is the one that uses TCSPC (time-correlated

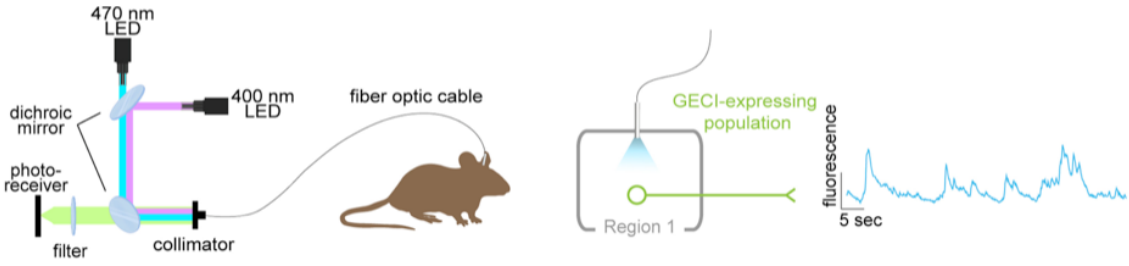

Figure 2.8: Fiber photometry system: LEDs, photoreceiver and dichroic mirrors to excite GECI and to collect the light emitted back by the fluorescent molecules [2]

.

single-photon counting)-based fibre-optic system [6]. The implanted fiber probe is tethered with the photometry system via two flexible fibers. A single-mode fiber is the mode to reach the fluorophore with excitation generated by the 473-nm picosecond-pulsed laser. The other fiber goes to a polychromator, which disperses the fluorescent emission into different directions and sends the input to a photomultiplier array to identify the single photons (Figure 2.9).

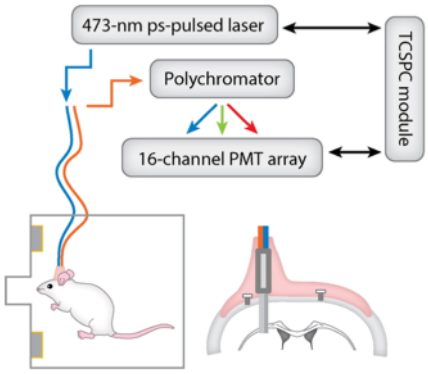

Figure 2.9: Example of fiber photometry system: two optical fibers, one for the deliver of the excitation light and one for the collection of the fluorescence emitted [6], [7]

.

In fiber photometry, the fluorescence collected reflects the neural activity of a the population of neurons expressing GECI, not allowing spatial resolution of single cells. The implanted fiber is tethered to the recording system with a fiber-optic path cable (Figure 2.8) and, when the technique in used with freely moving mice, the vibration of fiber during movements can cause noise to appear in the recorded signal. Also background autofluorescence and calcium signal distinction is tricky and, together with the inability to monitor the single cell, represents an important limit of this technique. On the other hand, this technique has key advantages, making it a good choice for *in vivo* applications. First of all, the reduced size and weight of the probes (diameter of 150-400 μm) make them suitable for recording multiple regions recording simultaneously, because more devices can be implanted in one animal above the region of interest with minim tissue damage. Further, the recording time is greater, because a lot less light is needed to excite the bulk population signal compared to other calcium imaging techniques and the fiber optics used are very sensitive in detecting light, so the intensity of excitation can be moderated reducing the problem of photobleaching. In addition to a very simple setup, photometry requires a reduced computational approach. The analysis of collected data demands a simple implementation and a not very large data storage. In fact, data obtained with photometry are 2-dimensional (fluorescence x time), instead in the case of single cell resolution, 3D data is necessary for the spatial information (fluorescence x space x time) [2].

For the advantages described above, in this work, a fiber photometry system has been implemented considering two variants of optical fiber.

Chapter 3

Materials and Methods

3.1 GCaMP6f

Neural activity causes rapid changes in intracellular free calcium. In general, genetically-encoded protein indicators are used to label specific cell types in order to study neuronal activity. GCaMP, in particular, is a genetically encoded calcium indicator (GECI) and it consists of a green fluorescent protein (GFP), a calcium-binding calmodulin (CaM) and a CaM-interacting M13 peptide, a peptide sequence from myosin light chain kinase. When the fluorescent protein is excited by light radiation at a specific wavelength, it is able to emit bright green light. But, when GECI bind to Ca^{2+}, there is an induction of a change in the fluorescence signal. This signal change allows measurements of action potentials, and other receptor activation events that trigger Ca^{2+} fluxes ([14]). Figure 3.1 shows how, when calmodulin binds to calcium, a conformational change causes an increase in GFP fluorescence.

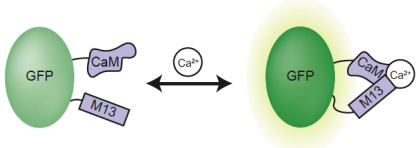

Figure 3.1: Calcium indicator GCaMP [1]

To express GCaMP selectively in the direct-pathway, adeno-associated virus vectors (AAV) expressing GCaMP6f (AAV1.syn.flex.GCaMP6f) were injected. Previous studies show that GCaMP6 indicators have a superior sensitivity than synthetic calcium dyes (for example,OGB1-AM) and identify single action potentials with high reliability. So these indicators are suitable to label spread groups of cells [6]. In particular, it has been demostrated that for characterization *in vivo*, among the family of GCaMP6 sensors, GCaMP6s, 6m and 6f have slow, medium and fast kinetics respectively but the more sensitive sensor is the one with slower kinetics. We chose GCaMP6f because it is the fastest genetically-encoded calcium indicator.

3.2 Animals and surgeries

All experimental manipulations have been performed in accordance with protocols approved by the Harvard Standing Committee on Animal Care following guidelines described in the US NIH Guide for the Care and Use of Laboratory Animals. The virus has been injected in D1-cre mice to express GCaMP indicators only in the direct-pathway neurons [6].

The first step of the experiment is performing a stereotaxic surgery that allows, through an access to the brain, virus injection and device implantations. After a sterilization of the working equipment and surgery tools, the mouse is anaesthetized with isofluorene, an inhalable gas anesthetic. The mouse is placed in a small chamber where isofluorane is released for few minutes (1-3 min) and then moved on to a stereotaxic instrument, like the one in Figure 3.2, with a mask positioned on the its nose to keep the animal anethetized during the procedure.

The stereotaxic instrument allows the mouse's head to be kept in a precise orientation for all the time [1]. At this point everything is ready for the brain exposure. The incision site is cleaned and sterilizated properly before cutting away the skin. Then, the skull is exposed and, once it is sufficiently dry, two visible anatomical

Figure 3.2: Stereotaxic instrument [8]

landamarks on the skull (lambda and bregma) are detected. Lambda and Bregma are two of the three reference points of the Stereotaxic coordinate system. They are the intersections of bone plates on the dorsal skull surface [15]. Bregma is defined as the intersection between the sagittal and coronal sutures of the skull and lambda is defined as the intersection between the lines of best fit through the sagittal and lambdoid sutures [1]. Figure 3.3a shows the top view of a rat skull, with lambda and bregma marked. From these visible reference points on the skull, the brain structures are located using three coordinate axes: Anterior-Posterior, Medial-Lateral and Dorsal-Ventral. All the stereotaxic coordinates are obtained from a stereotaxic atlas (Figure 3.3b), a 3D reconstruction of the brain with serial sections and drawings of the sectioned brain ([16]). To target the brain regions, the mouse is positioned onto the stereotaxic instrument and the skull must be flat in order to have lambda and bregma aligned in the rostral-caudal direction.

The last step to expose the brain is craniotomy: a dental drill makes small holes in the skull in the regions of interest for the implanting of the devices or the injection of the virus.

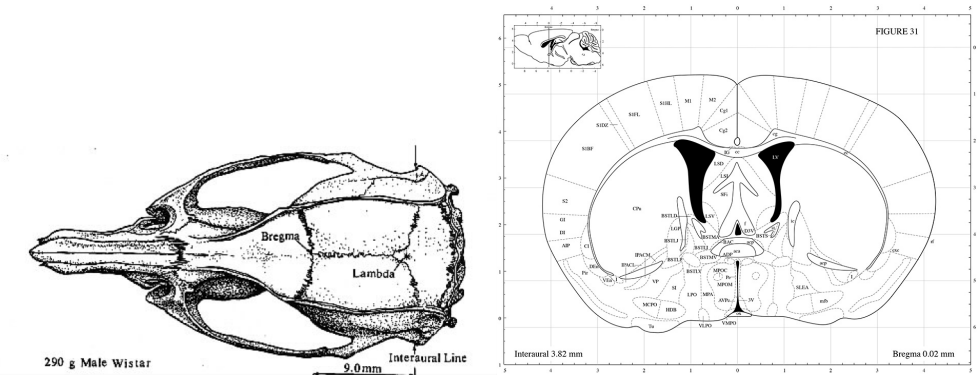

(a) *Dorsal view of the skull [15]* **(b)** *Example of stereotaxic atlas [16]*

Figure 3.3: Stereotaxic coordinates are obtained from a stereotaxic atlas. All the coordinates for locating brain regions are calculated as the distance from two visible reference points on the skull: lambda and bregma.

3.3 Behavior

Important in studying the role of brain areas in the control of movements is to associate the recorded neural activity with a period of time in which the movement is carried out, from initiation to the actual action.
In this work, the neural activity for the direct pathway in the striatum has been studied for self-initiated movements. A self-timed paradigm is appropriate to analyze the role of neuronal populations in the generation of movement, becuase it allows us to look at neural activity when the same movement is performed and clearly separated from proximal sensory cues. Thus neural activity related to the behavioral process of interest can be clearly isolated. Mice are trained to make the same movement triggered by an external cue. They learn to respond the cue not immediately but after a certain delay that they choose themselves; in this way, even if actually induced by an external cue, the movement starts spontaneously from the mouse and is not a simple reaction to a stimulus.

Behavior training and optical mueasurements have been executed in an experimental rig. In this chamber, the mouse was on a platform and head-fixed to keep

the animal stationary. A touch-sensitive tube was located just under the mouse's mouth. This tube has a sensor that allows it to detect whenever the mouse touches it. The mice have been trained to perform an interval timing task that requires the animals to lick the tube after a visual and sound stimulus. At the beginning, the rig is in the dark. After a certain time interval, which can range from 400 to 1500 ms, a visual stimulus and a pure tone (3300 Hz) are used as cue to initiate timing. The mouse will be juice rewarded only if he licks in the "operant window" that starts 3.33s after the cue and remains until 7s. Only the first spontaneous lick will be rewarded. The mouse can trigger the reward if it licks in the operant window and if he doesn't lick in the "no-lick window" that precedes the operant one. Abort window starts 400 ms after the cue; if the mouse licks before 3.33 s after the cue, he will not get rewarded and an error tone is played at the same time that the lamp turns on. There is one more interval, the "post-cue interval", lasts for 400 ms after the cue and allows the mouse to not abort the current trial if he licks in this time since it is frequent that mice have impulsive licks right after the cue.

3.4 Fiber Photometry Setup

Photometry allows us to record the activity of genetically defined neural populations in behaving mice by expressing a genetically Ca^{2+} indicator GCaMP6f and chronically implanting an optic fiber. A general single fiber photometry system consists of an excitation light source, a fluorescence cube and a photodetector. The used experimental setup is shown in Figure 3.4, in which the delivery and collection paths for excitation and emission light in the system are highlighted:

- **LED Driver** (PlexBright^{TM} LD-1 Single Channel LED Driver) used to hand adjust the amount of light the LED Module outputs. The actual current (in milliamps) is shown on the Output display.

- **LED Module** (PlexBright Table-Top LED Modules) generate and couple high-intensity light into an optical fiber. Blue light (465 nm) has been used during the experiments.
- **Fluorescence Mini Cube with 3 ports**, that has a dichroic mirror to separate the excitation light from the fluorescence emission [17].
- **Photoreceiver Module** receives the fluorescence emitted by the neurons and converts the optical flux signal into measurable electric voltage between 0 and 5 V.

When the laser beams enter in the fluorescence mini cube, they are reflected by a dichroic mirror and launched into the core of a multi-mode optical fiber patch cable [18]. The distal end of this patch cable in connected to an implantable optical fiber probe. The emission fluorescence collected form the fiber probe comes back along the path cable, passes by the dichroic mirror and is launched in to the photodetectord module.

3.5 Cut Fibers in D1

To record the neural activity from the direct-pathway, a multimode optical fiber was implanted in D1-cre mice after the injection of a AAV virus expressing GCaMP6f as protein indicator. The protein indicator permits us to indentify only dSPNs and, through a multi-mode optical fiber, neurons are lighted up and the fluorescence emitted is collected. A surgery procedure with two main steps is required: stereotaxic AAV injections to express proteins in taget brain regions and the implant of the optical fibers. In this experiment both the injections and the fiber implant were performerd in the dorsal striatum.
Two craniotomies were made bilaterlally in two adult mice. In particular the craniotomy locations are anteroposterior 0, mediolateral +2.6 mm (left), -2.6 mm (right)

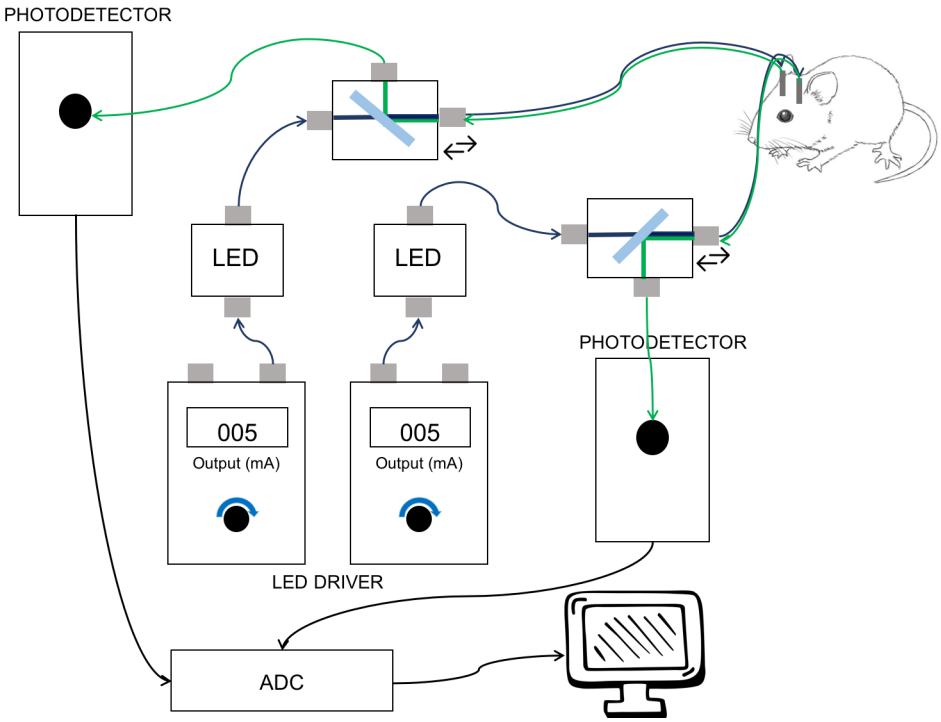

Figure 3.4: Experimental photometry setup

from bregma. In these positions, two holes were drilled and a total volume of 100 nL of AAV1.Syn.Flex.GCaMP6f.WPRE.SV40 ($2.54 \cdot 10^{13}$ $\frac{gc}{mL}$) vector per site was injected. Subsequently, two multi-mode optical fibers (NA=0.53, total length=4 mm) were slowly lowered from the surface of the brain until 2.311 mm ventral. The implants were fixed with metabond and an headpost was cemented to fix the mouse in the rig during the phases of behavior and recording (Figure 3.5).

3.6 Silk-Coated Tapered Optical Fibers

The same experiment was then repeated with novel tapered fibers that have several advantages over standard cut fibers. The surgery procedure has been simplified using a new technique to label the neurons. In particular these innovative fibers have been coated with a polymer mixed with virus and able to release it once the

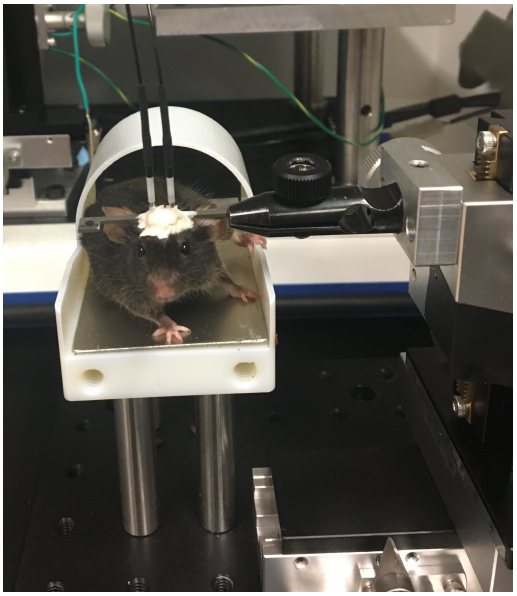

Figure 3.5: Mouse with the headpost ready for training

fiber has been implanted. This new technique allowed us to avoid the injection step during the surgery, shortening the time and limiting the probability of demaging the tissue.

3.6.1 Tapered fibers

Flat optical fibers used to illuminate brain regions have the same diameter along the whole length and a flat endface perpendicular to the longitudinal axis of the fiber [19]. They are placed above the region of interest and illuminate a spherical volume around their end-surface, but, because of attenuation by the tissue, to light up neurons ∼100 μm away from the emitting point, an increase of the laser power is necessary. Moreover, the end of the fiber is blunt and large, causing a tissue damage during its insertion in the brain [9].

Tapered fibers are innovative devices whose geometry allows to overcome limits of the standard fibers pointed above. They are multimode fiber optics with a length that ranges from 1.5 to 5.6 mm and a diameter that decreases along the fiber ending

like a tip. In fact, the section perpendicular to the longitudinal axis tapers from 125-225 μm to $\sim$500 nm at the end. Depending on the length and the initial diameter, the taper angle changes between 2°and 8°. Figure 3.7a shows the geometry of a tapered optical fiber with a length of 4.4 mm, a core/cladding diameter of 225 μm and a taper angle equal to 2.9°.

Tapered fibers limit invasiviness and tissue damage when inserted in the brain because are smaller than the flat ones with a reduced cross-section. They can be put in the region of interest and not above it, because light delivery takes place mainly from the sides of the fiber, and are able to illuminate more homogeneously large areas in the brain or small controlled sites. The first case occurs when the light enters in the fiber using the full NA allowing uniformly illumination along the all length (Figure 3.6a). In fact, the light-emitting segment (L) depends on the taper angle considering a fixed NA. L can range between few hundred micrometers to a few millimeters considering 0.22 and 0.39 NA fibers with ψ from 2.2 °to 7.4 °[9]. Figure 3.6b shows both the flat and the taper fibers implanted. The two fibers light up a different quantity of neurons and this happens for two reasons:

- the tapered fiber emits light also along its length and not only at the endsurface, covering an area of the cone defined by L and ψ.
- the angle, formed with the fiber axis, from which the light emerges, is different from zero, and so tissue absorption and scattering determine light distribution along the direction of emitted light, which has a component along the fiber axis, as for the flat fibers, and a component perpendicular to the axis.

Therefore, illumination of larger areas is possible by choosing fibers with NA and geometric characteristics that allow us to obtain the required lighting, without necessarily increasing the power of light entering the fiber.

It is not necessary to use the entire length of the fiber for the emission of the light in fact, varing the ray input angle permits selection of different output sites

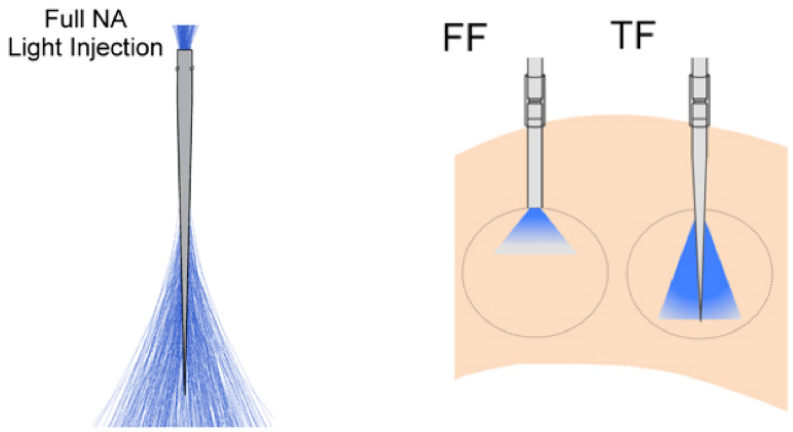

(a) *Full NA of the fiber used to inject the light.*

(b) *Different illuminated areas with flat fiber and tapered fiber*

Figure 3.6: Light injected into the fiber using the full NA [9].

along the fiber [9]. In Figure 3.7b the three different output spots derive from three distinct angles of the light in input to the fiber (θ). When θ increases, the emitting point is farther from the tip. The injection angle depends on the NA and on the taper angle of the specific fiber.

3.6.2 Silk Fibroin Solution

To label neurons with a molecule that has calcium-dependent fluorescence, a virus is normally injected into an area of the brain through a small hole in the skull. This requires that the surgery procedure has two basic steps, one to inject the virus and one to implant the fiber. Both steps are invasive and physically perturb the brain, increasing the probability of damaging the tissue. Furthermore, to have good chances of success, the point of virus injection and the implant position must be aligned. The risks of failure of this procedure are high and this entails a greater probability of an increase in costs and time [11].

Coating the fibers with films made of silk fibroin and AAV vectors avoids the

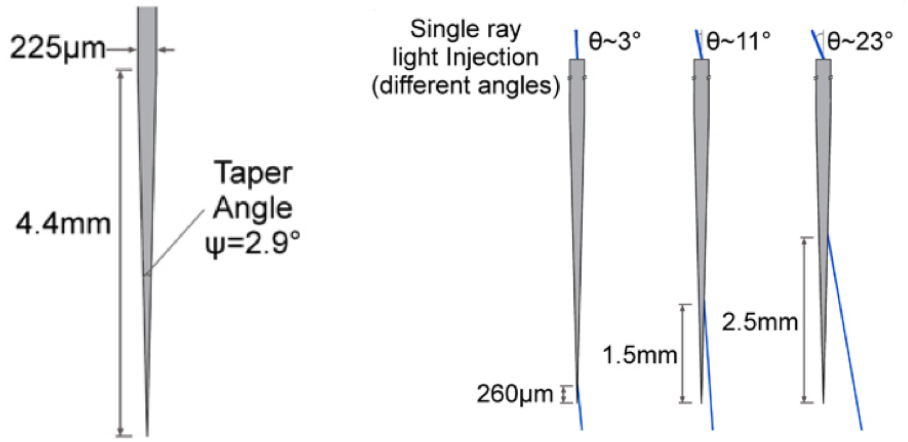

(a) *4.4 mm long tapered optical fiber with ψ equal to 2.9° and core/cladding diameter of 225 μm*

(b) *Three different emission spots from the same tapered fiber varying the angle of injection of the light*

Figure 3.7: Examples of light emissions from tapered fibers [9].

injection step and at the same time obtains a uniform distribution of the virus along the whole fiber [11]. Have a uniform expression of the virus over the whole extension of the device is essential to make better use of the ability of fiber to illuminate selective regions around its length.

The film used for the coating is a mixture of a silk fibroin solution with AAV-GCaMP vector; silk fibroin is a polymer purified from domesticated silkworm (Bombyx mori) cocoons with several interesting features for immobilization [20]. Silk has been demonstrated to have excellent mechanical properties, biocompatibility and optical properties [20]. It is also able to encapsulate viral vectors and release them into tissue after implantation [21]. Tapered optical fibers with NA of 0.66 and length of 2 mm were used instead of flat-cleaved ones. For the coating a silk solution was 1:1 mixtures of silk fibroin and AAV1.Syn.Flex.GCaMP6f.WPRE.SV40 ($2.54 \cdot 10^{13}$ $\frac{gc}{mL}$). The silk tapered fibers have been implanted in the same locations of the cut fibers (anteroposterior 0, mediolateral +2.6 mm (left), -2.6 mm (right) from bregma)

and have been lowered for 4.5 mm from the surface of the brain to position them inside the striatum and not above as previously.

3.6.3 Localized Light Delivery

Tapered fibers allow selective illumination of the region around them by varying the angle at which light is injected into the fiber. A simple method for changing this angle requires an easy optical setup in which, with a lens and a translating mirror, the light input direction can be varied [9]. Figure 3.8 ([10]) shows an aspherical lens and a mirror located between the laser beam and the tapered fiber. The mirror can translate along the direction of beam propagation and focuses the light at the input facet of the fiber with a different input angle θ =arctan $\left|\frac{t}{f}\right|$ depending on its position. When mirror is at the zero position the laser beam is focused into the fiber witouth deflection.

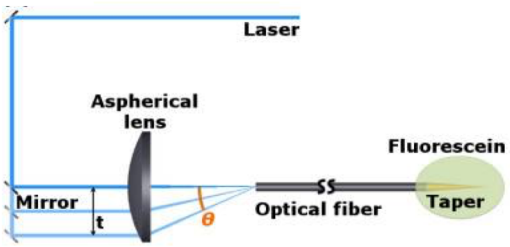

Figure 3.8: Optical setup to select different output sites from the fiber [10].

In the experiment the ThetaStation-1 (from Optogenix S.r.l.) has been used for "*in vivo* selective illumination". It has been mounted between the LED Module and the dichroic mirror in the photometry setup only for the left side illumination. The ThetaStation-1 box has two ports, one for the input laser beam directed to the lens and one for the output direction of the beam after its deflection; a micrometric screw is used to manually translate the mirror along the input beam direction. A

calibration step is necessary because the emitting sub-portion of the fiber and the power of the light emitted change according to:

- the geometric characteristics of the fiber
- the light source used
- the input and output patch cables used

Therefore, depending on the conditions of use, to obtain sufficient illumination to record the neural activity, the position of the micrometer screw is different. The calibration has been exectuted using tapered fiber with geometric characteristics equal to those implanted. The light moves along the fiber just turning the screw manually . For a screw position at zero, all light is concentrated in the fiber tip. By increasing the position of the screw, the light flows along the entire length of the fiber; once the position of emitting segment (L) is reached, a decrease in light intensity is noticed if the position is increased further. On these evidences a screw calibration was performed with tapered optical fibers (NA of 0.66 and length of 2 mm) obtaining for a position of the screw equal to 0, light concentrated at the tip of fiber and for postition equal to 14 the light concentrated at the bottom.

3.7 Data Analysis

The electric output signal of the photoreceiver ranges between 0 and 5 V and it represents the fluorescence related to the calcium flux. Raw traces need to be represented in a more explainable unit system. The raw values have been manipulated to express change in fluorescence over the average fluorescence of a given time period, and dF/F has been calculated. Usually, the way to do that is to define dF/F as in (3.1): where F is the intensity of signal at a certain time and F_0 is the average

intensity across the entire acquisition session [2]. This is repeated for each value of F in the entire recording.

$$\frac{dF}{F} = \frac{F - F_0}{F_0} \tag{3.1}$$

Another approach to represent dF/F is to change the term of normalization and use as F_0 the value of the baseline calculated across 10 trials. Representing the change in fluorescence instead of the raw data allows to have the average of the entire signal equal to zero.Raw trace of a signal acquired in one session recording is shown in Figure 3.9. The fluorescence intensity (V) is plotted over time (s) from left-side optical fiber for one mouse. The raw trace is smoothed (Figure 3.10) using a moving average filter with a span of 10 trials (200 s). Figure 3.11 shows the raw signal and the smoothing for the entire trace. Then smoothing is subtracted from the raw signal and the output signal is normalized with the smoothed one obtaining the dF/F signal with average equal to zero (Figure 3.12). If the dF/F is zoommed on the trial number 15, a peak is evident right after the first lick of the trial (Figure 3.13).

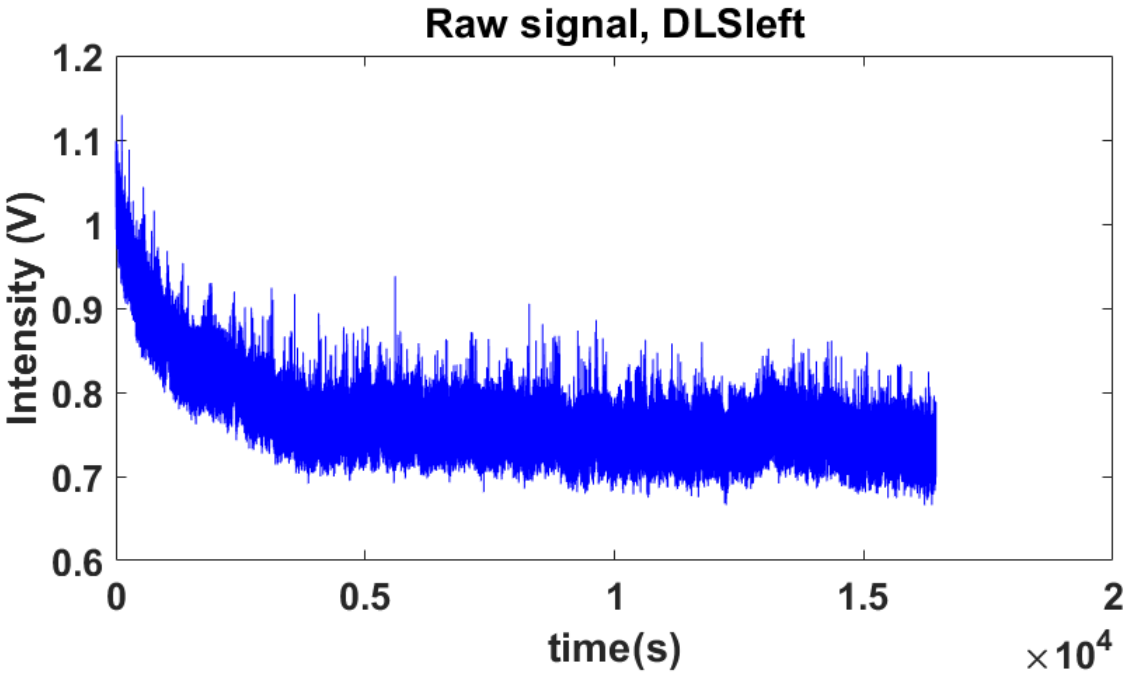

Figure 3.9: Fluorescence signal recorded in one day.

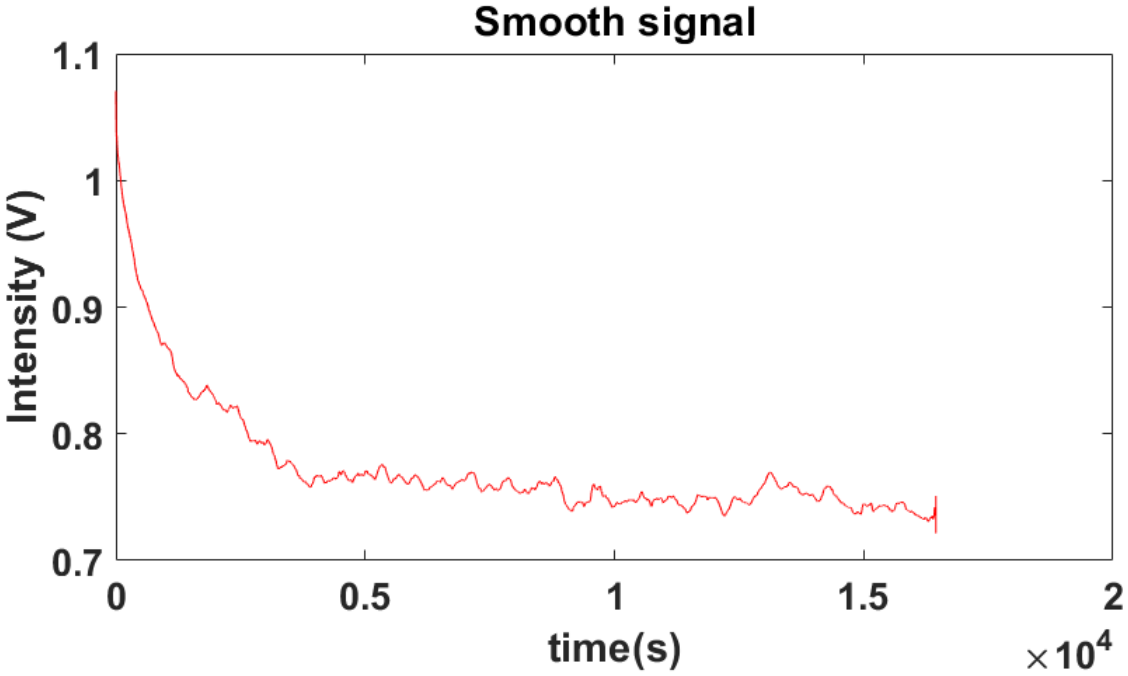

Figure 3.10: Smooth of raw signal

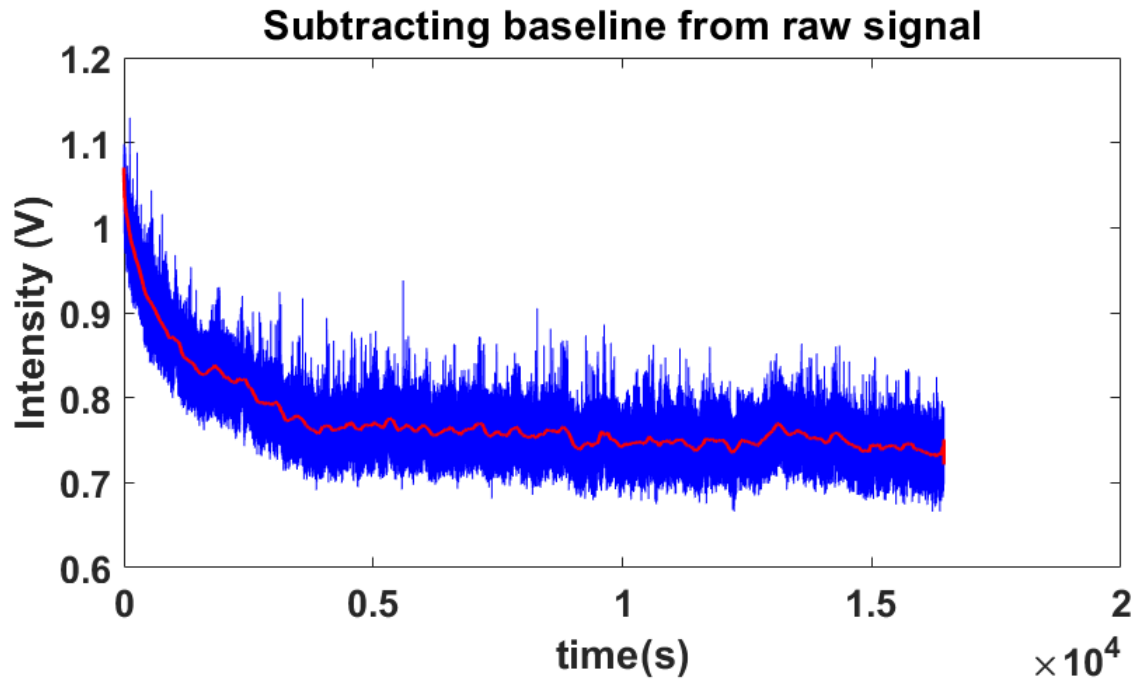

Figure 3.11: Raw trace and baseline over time for one session.

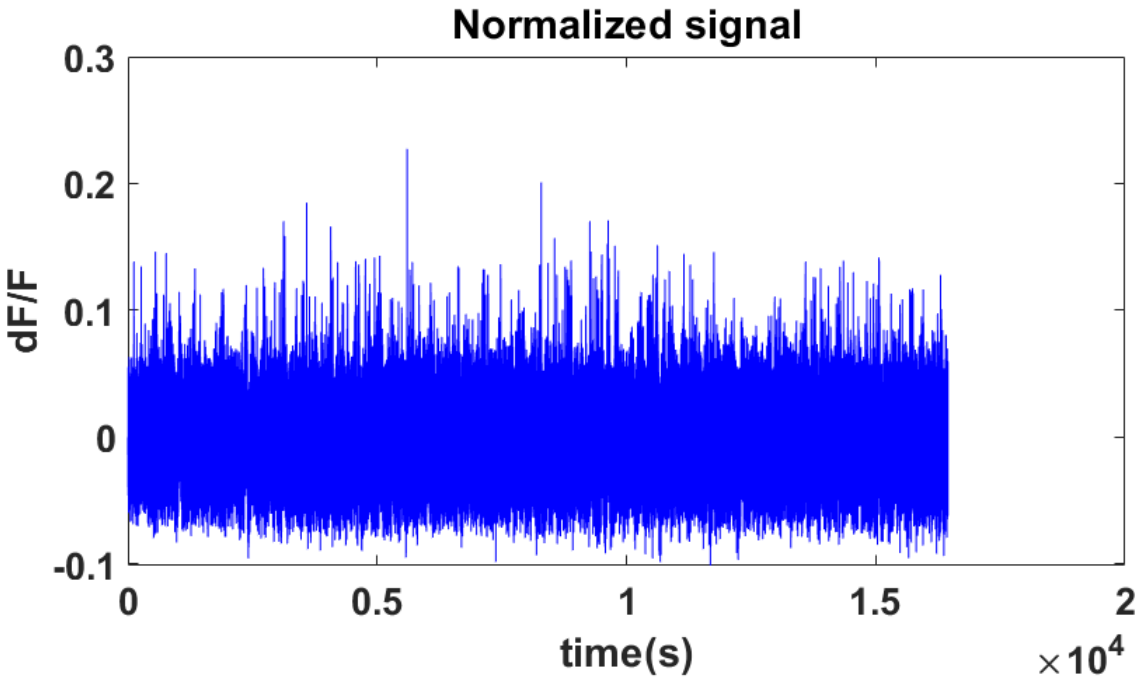

Figure 3.12: dF/F signal for one recording session.

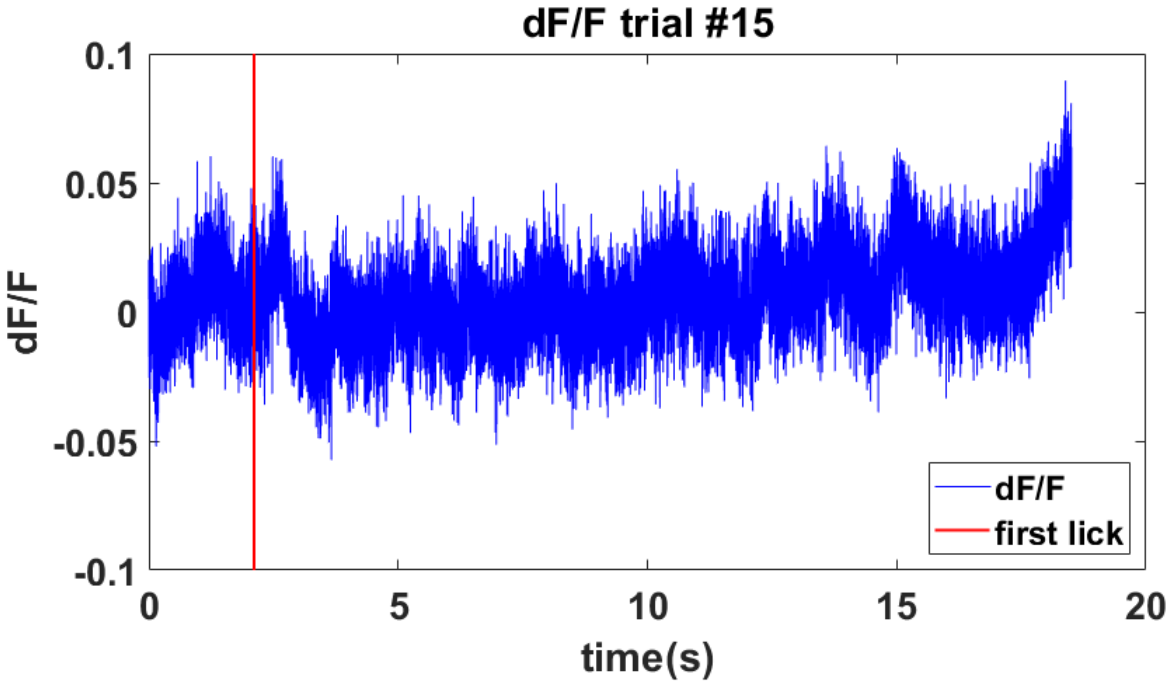

Figure 3.13: dF/F signal for one trial of one day recording.

Chapter 4

Results

4.1 Cut Fibers

In two D1-cre mice, flat optical fibers have been implanted bilaterally in the dorsal striatum. Figure 4.1 and Figure 4.2 show the expression of GCaMP6f in the striatum, for mouse 1 and mouse 2, two months after the injections. The virus spread out around the fiber and reached also the cortex.

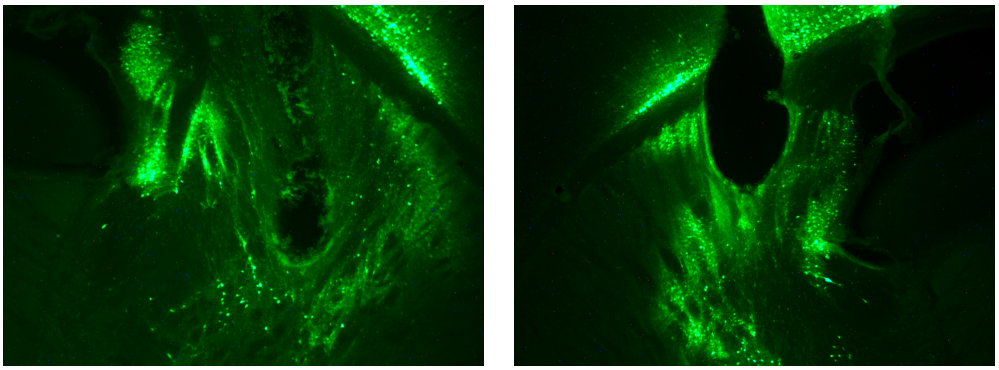

(a) *Mouse 1 - left* **(b)** *Mouse 1 - right*

Figure 4.1: Images of striatum histology for mouse 1.

Per each mouse, dF/F signal has been calculated on a trial by trial basis over

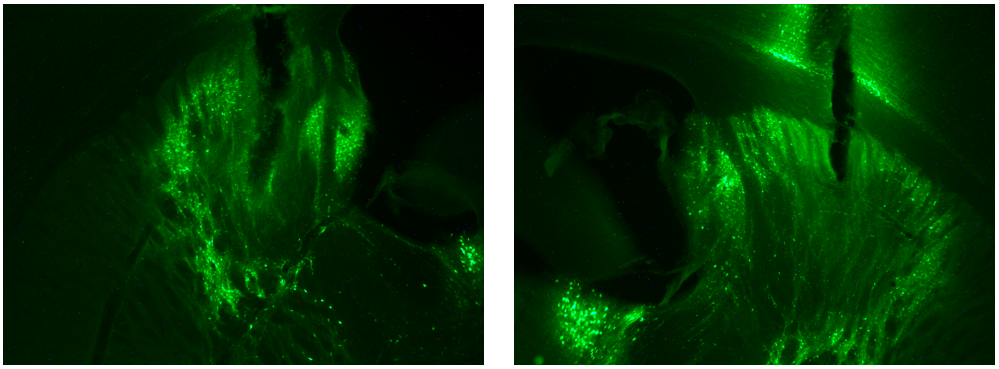

(a) *Mouse 2 - left* **(b)** *Mouse 2 - right*

Figure 4.2: Images of striatum histology for mouse 2.

the entire session for GCaMP6f fluorescence. All the signal analysis is done separating trials in which the mouse got rewarded from those in which it licked early, aborting the rewarding. Fluorescence changes are represented averaging signal over all sessions for each mice. Since the goal is to analyze the neural activity related to the specific behavior, here the important thing is see what happens before the spontaneous action. Therefore the dF/F signal around the "decisive" lick (time zero in the plot) is represented from 7 s before the lick to 4 s after. Figure 4.3 and Figure 4.4 shows dF/F signal for rewarded and early trials over all sessions for left-side fibers in both mice. From a baseline that indicates very low activity, 3-2 s before the lick a transient leads to a decreasing of the activity. At the moment of the lick, the signal crosses ordinates showing an increase in activity with a peak few ms after the lick and then a transient carries the signal back to a baseline. In case of rewarded trials, the baseline stabilizes around 20% of the peak value. For mouse 2, it seems that there is again an increasing of the activity 2s after the lick. This new ramp can derive from the behavior performed by singolar mouse; sometimes animals start licking at high frequency after the juice reward even if there is no more juice released. For the aborted trials, the signal trend is similar to previous cases, but, after the peak, activity decreases and then 2 s later comes back to the zero baseline.

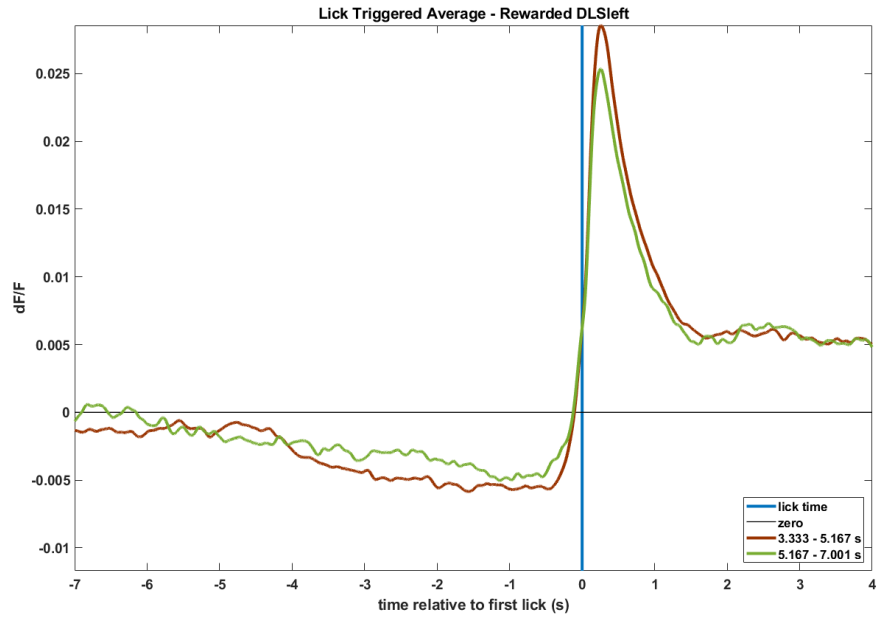

(a) *Mouse 1, 739 trials*

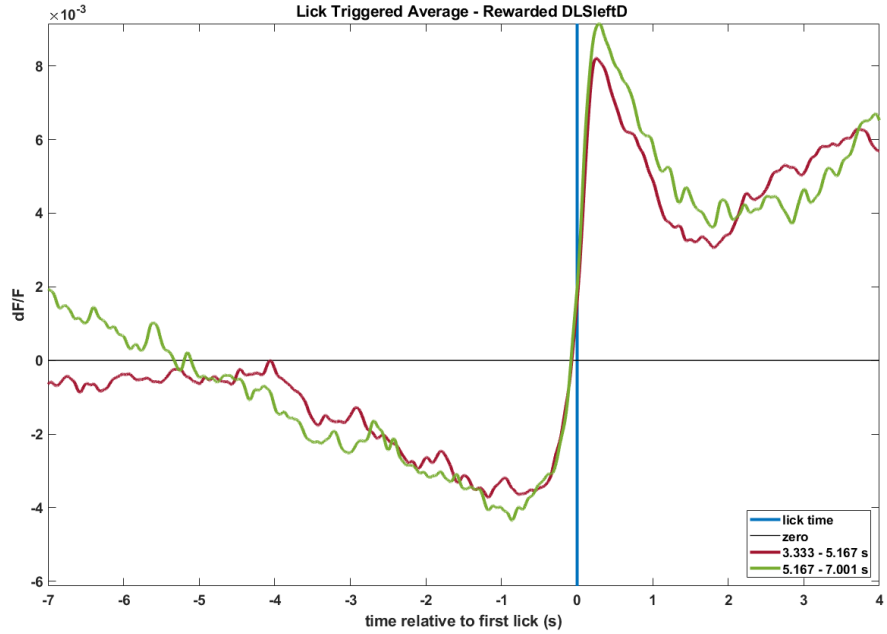

(b) *Mouse 2, 1026 trials*

Figure 4.3: dF/F signal from fiber implanted in the left dorsolateral striatum for rewarded trials in mouse 1 and mouse 2.

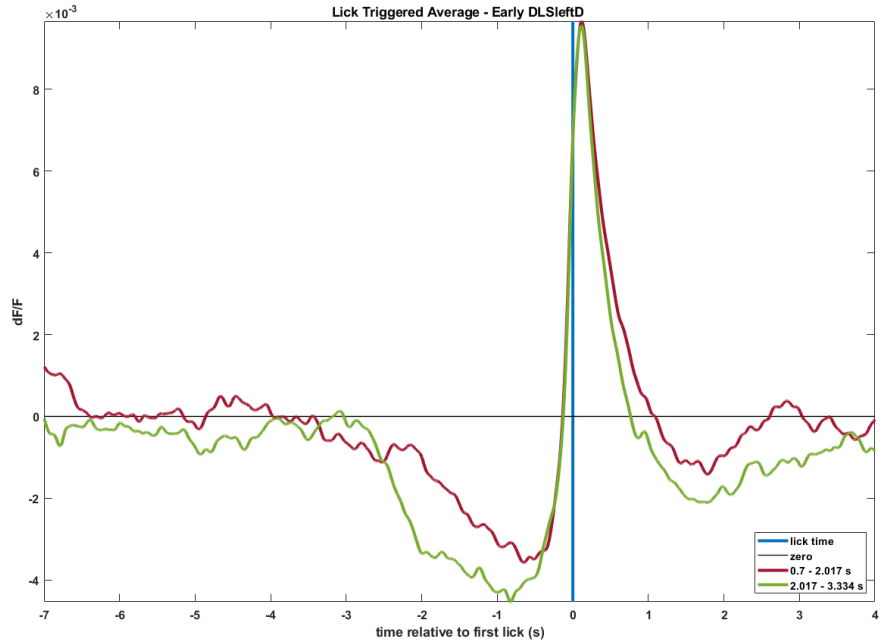

(a) *Mouse 1, 1957 trials*

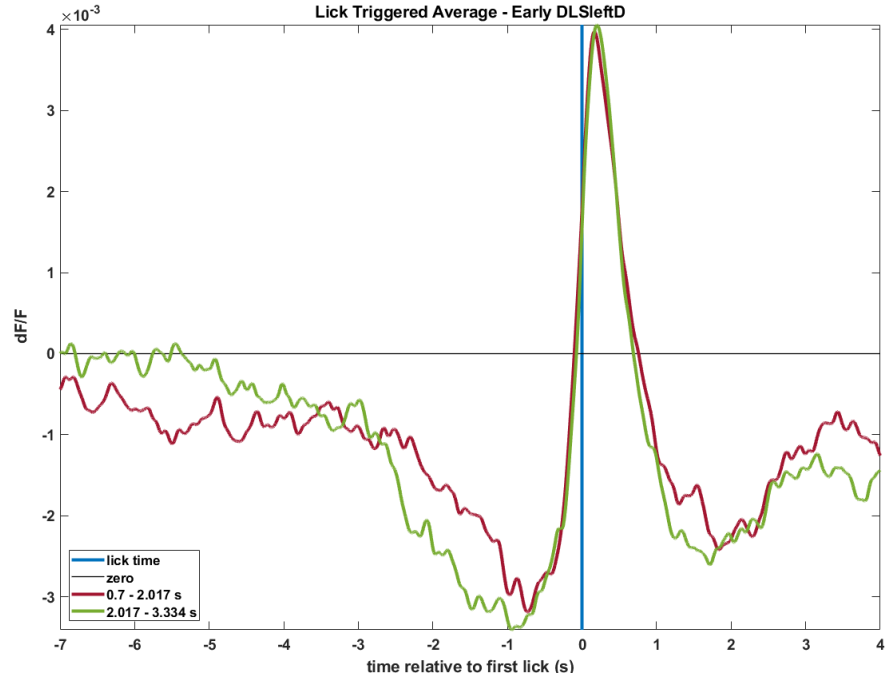

(b) *Mouse 2, 2321 trials*

Figure 4.4: dF/F signal from fiber implanted in the left dorsolateral striatum for early trials in mouse 1 and mouse 2.

The dF/F for the right side has similar shape to the previous case for mouse 2, in both rewarded and early trials (Figure 4.5 and Figure 4.4). A very different pattern is shown for mouse 1. From the histological images, GCaMP6f is expressing in the striatum and the different signal obtained from neural activity could be due to a broken optical fiber or to neurons damaged.

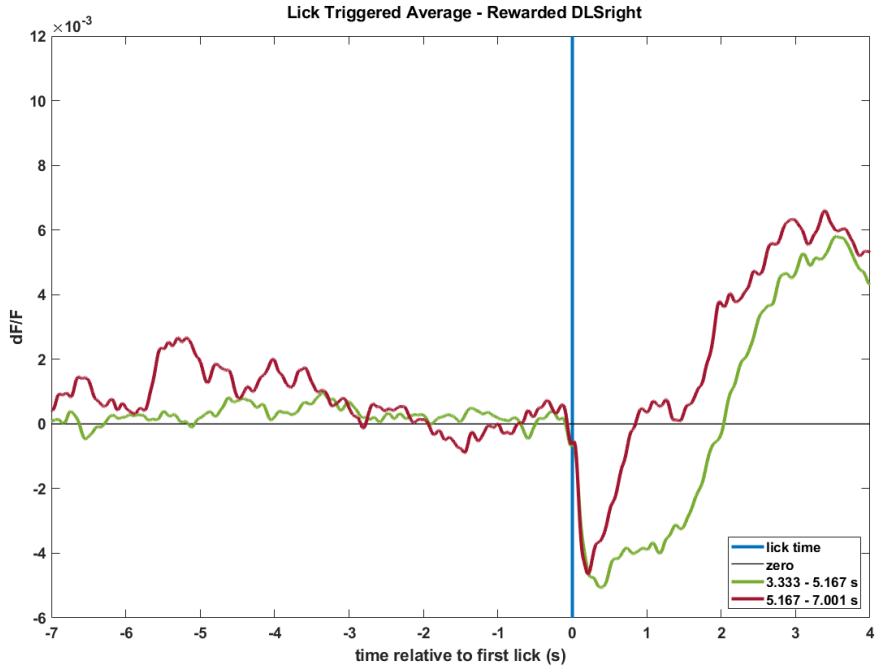

(a) *Mouse 1, 739 trials*

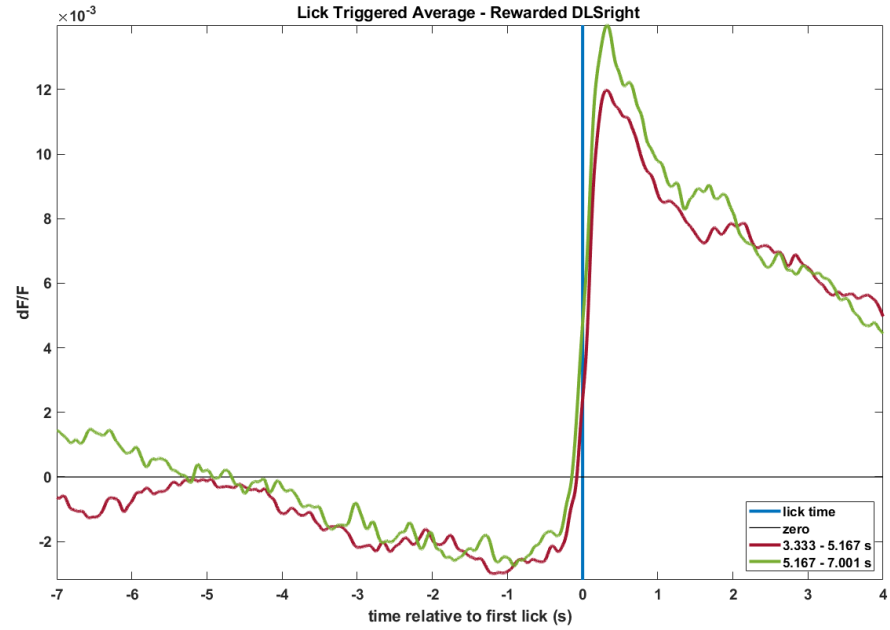

(b) *Mouse 2, 2016 trials*

Figure 4.5: dF/F signal from fiber implanted in the right dorsolateral striatum for rewarded trials in mouse 1 and mouse 2.

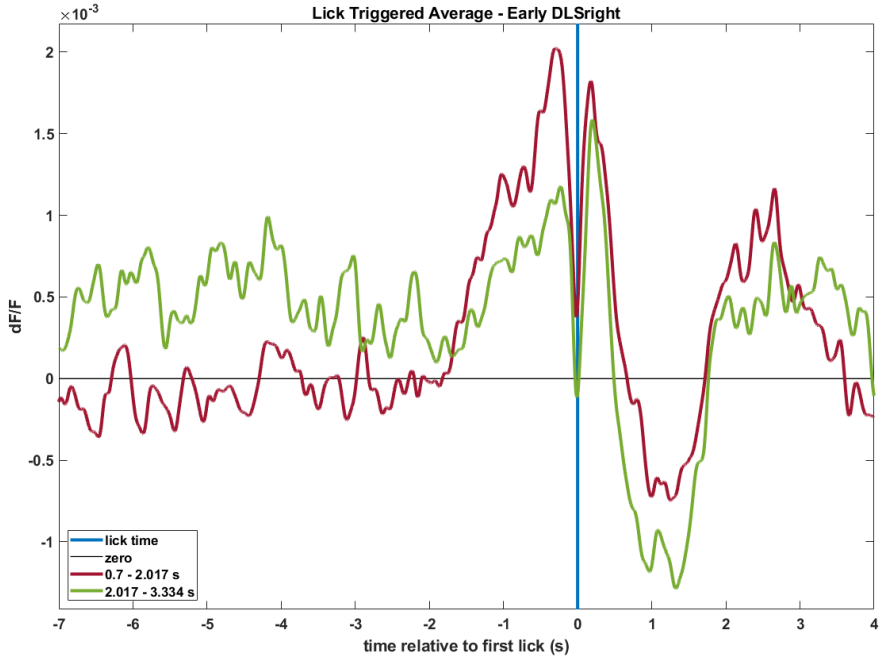

(a) *Mouse 1, 1957 trials*

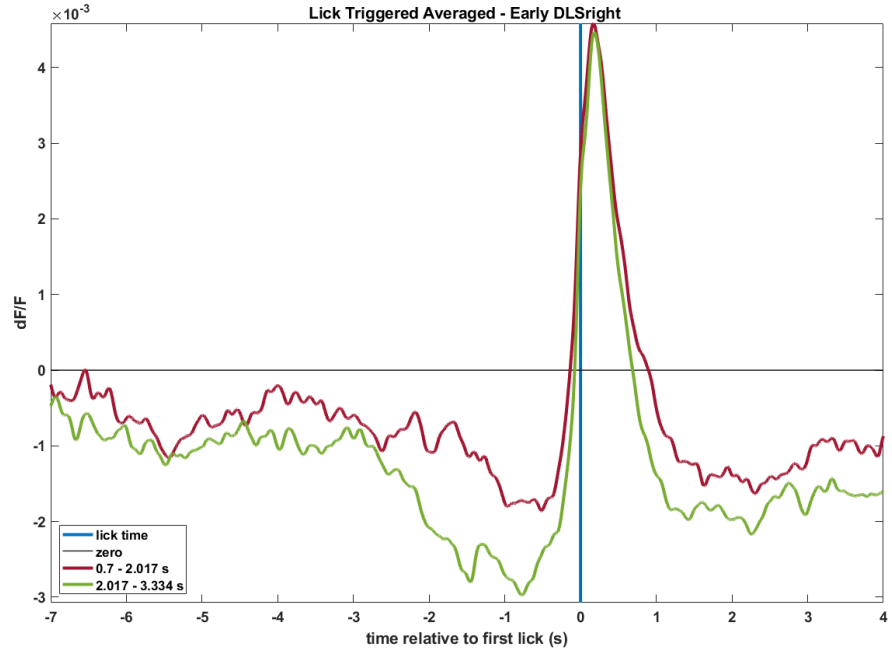

(b) *Mouse 2, 2321 trials*

Figure 4.6: dF/F signal from fiber implanted in the right dorsolateral striatum for early trials in mouse 1 and mouse 2.

4.2 Silk Tapered Fibers

Two silk tapered fibers have been implantend bilaterally in three D1-cre mice: mouse 3, mouse 4 and mouse 5. Figure 4.7 shows the histology pictures of striatum for mouse 5. If compared with the previous ones in case of virus injection, the expression is very low. The GCaMP expression is concentrated in the cortex instead of in the striatum (Figure 4.7). The reason could be that, during the implant of the fiber, the polymer was not dry enough, and, when the ensemble fiber and polymer was lowered in the brain, silk solution remained concentrated in the cortex. Looking at dF/F signal for mouse 5, Figure 4.9 shows an amplitude of the dF/F so low that can be defined as noise. Below, dF/F plot is represented for the other two mice (mouse 3 and mouse 4) with silk-coated tapered fibers (Figure 4.10, Figure 4.11, Figure 4.12, Figure 4.13).

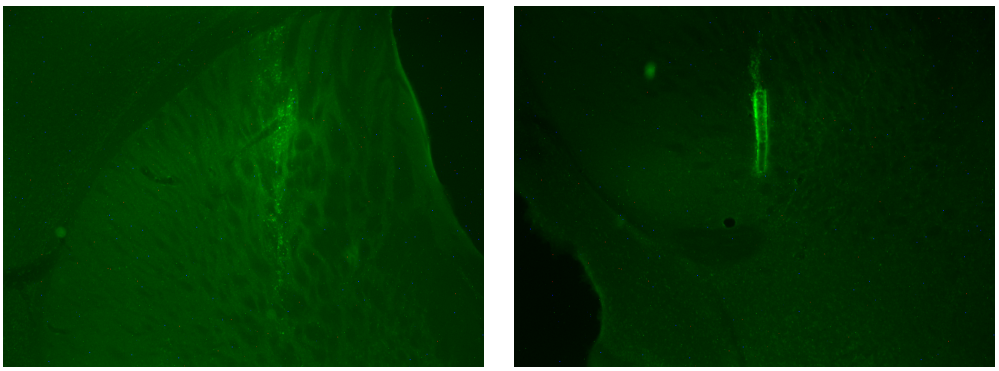

(a) *Histology of striatum and cortex for right side.*

(b) *Fiber implanted in the striatum*

Figure 4.7: Images of striatum histology for mouse 5 with only one fiber implanted in the right dorsolateral striatum

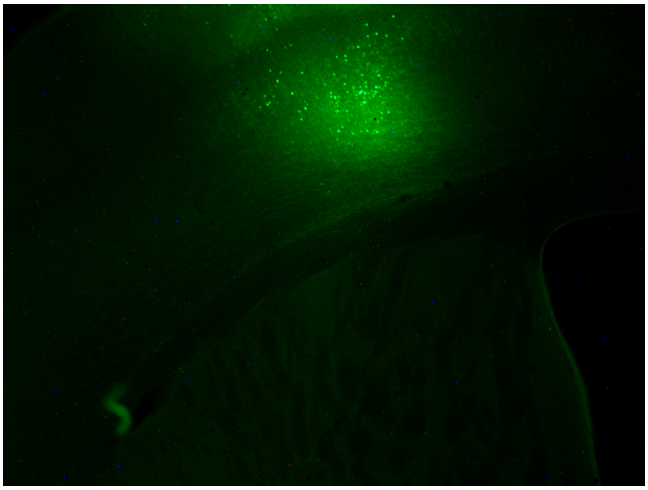

Figure 4.8: Mouse 5: GCaMP expression is visible in the cortex instead of in the striatum.

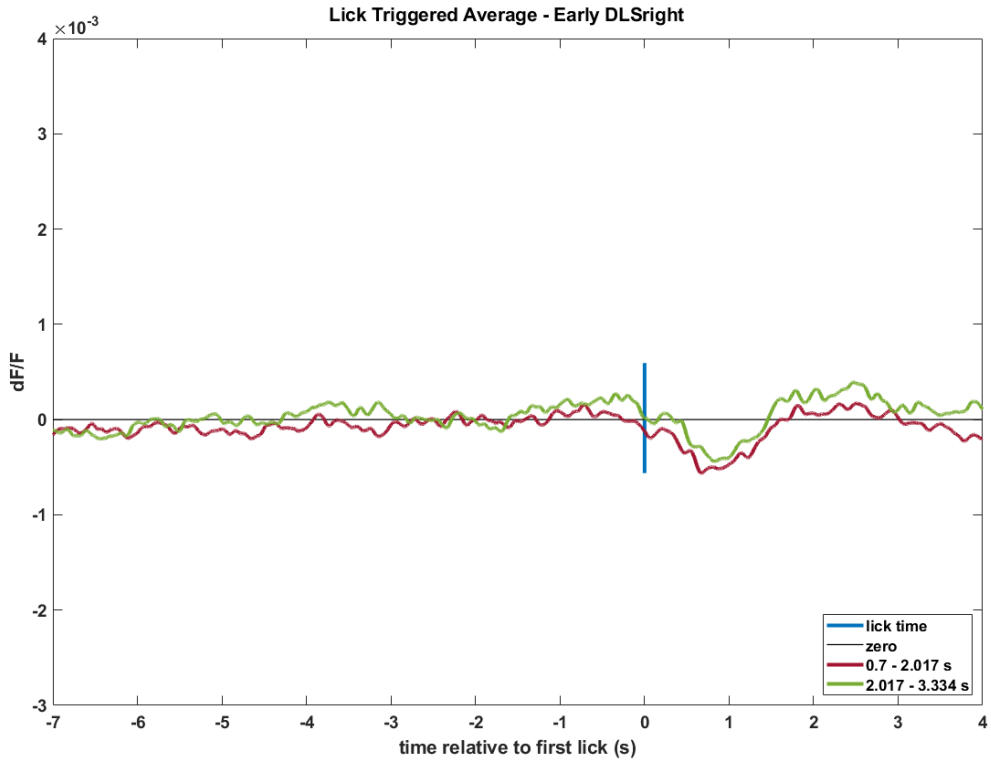

(a) *2621 early trials*

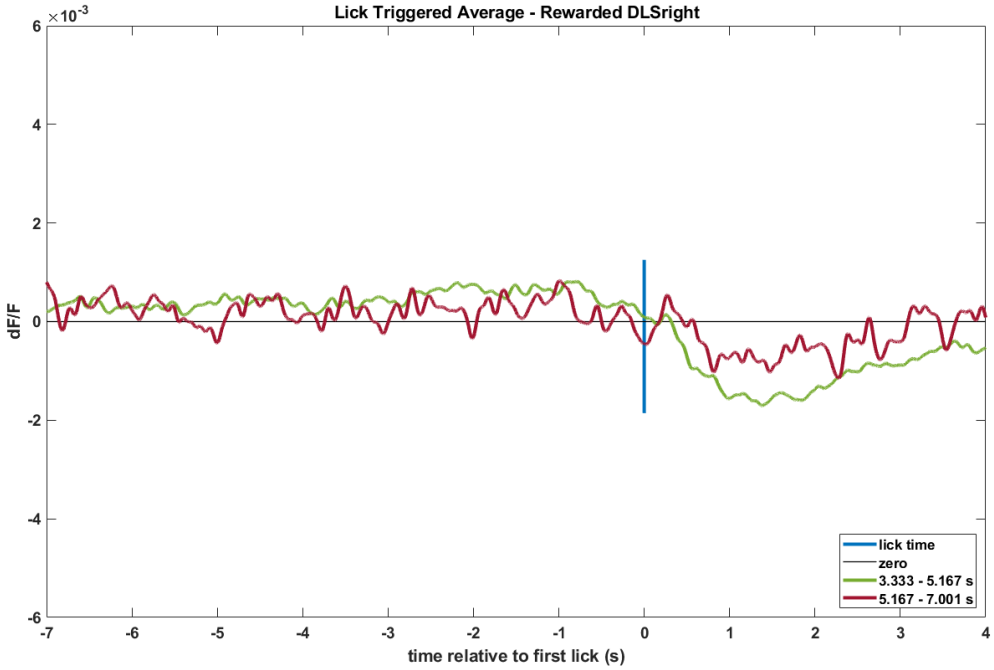

(b) *615 rewarded trials*

Figure 4.9: dF/F signal form fiber implanted in the right dorsolateral striatum for early and rewarded trials in mouse 5.

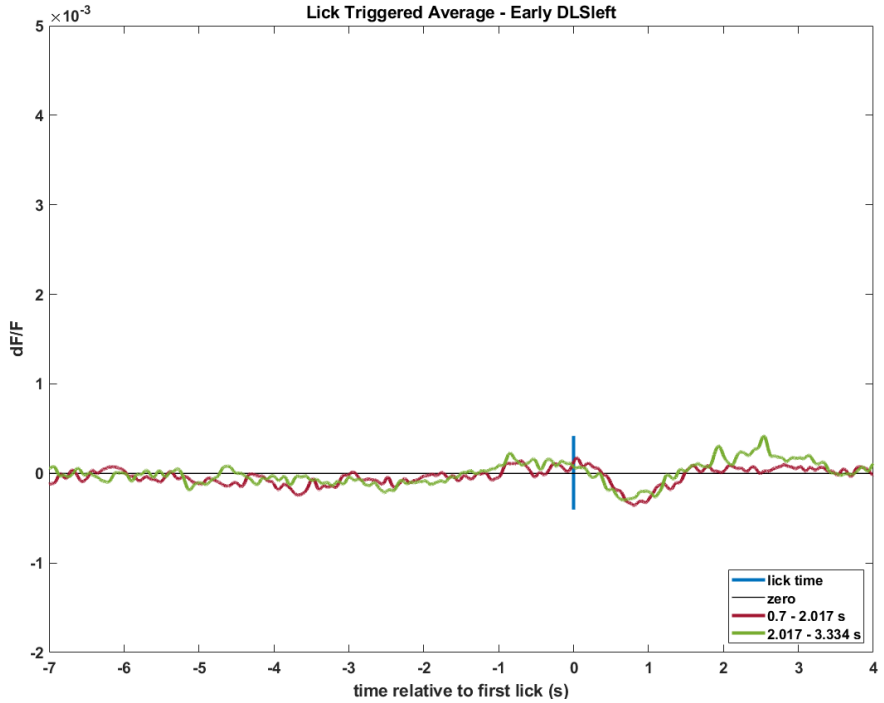

(a) *Mouse 3 - left side*

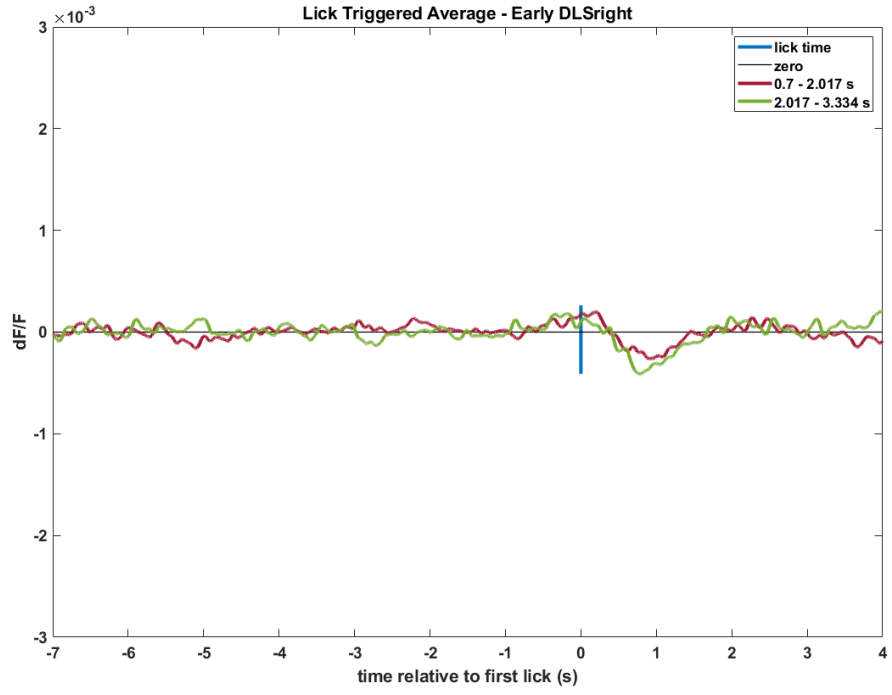

(b) *Mouse 3 - right side*

Figure 4.10: dF/F signal form fiber implanted in the right and left dorsolateral striatum for 1659 early trials in mouse 3.

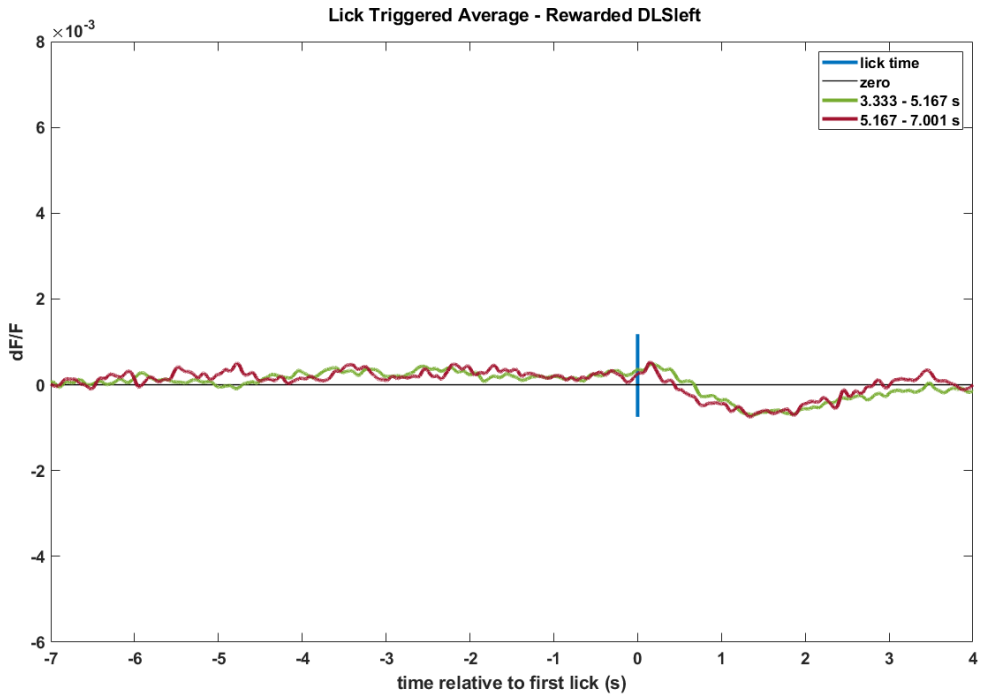

(a) *Mouse 3 - left side*

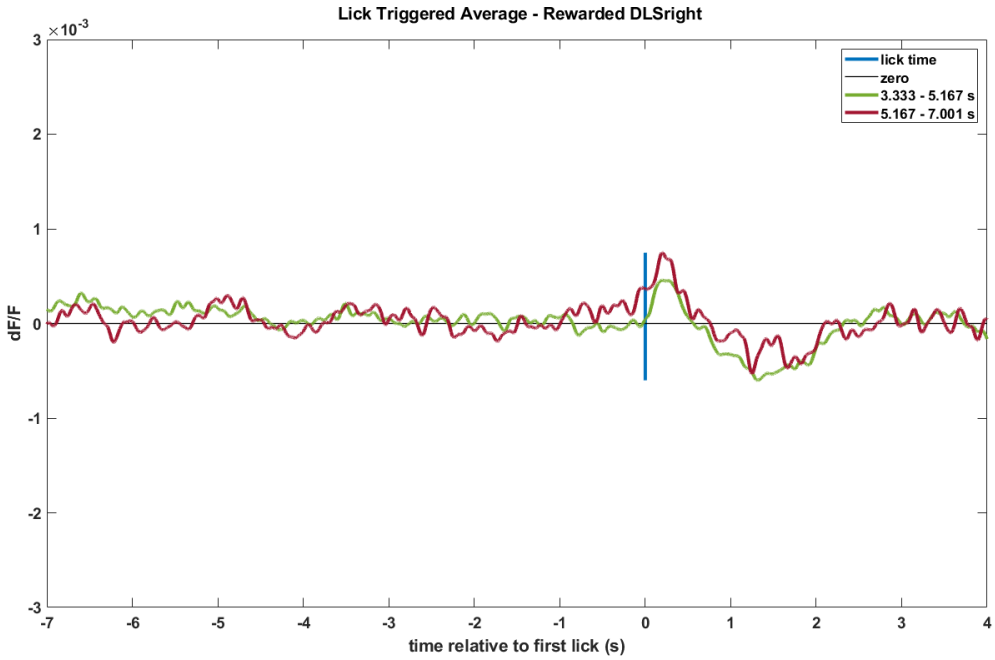

(b) *Mouse 3 - right side*

Figure 4.11: dF/F signal form fiber implanted in the right and left dorsolateral striatum for 530 rewarded trials in mouse 3.

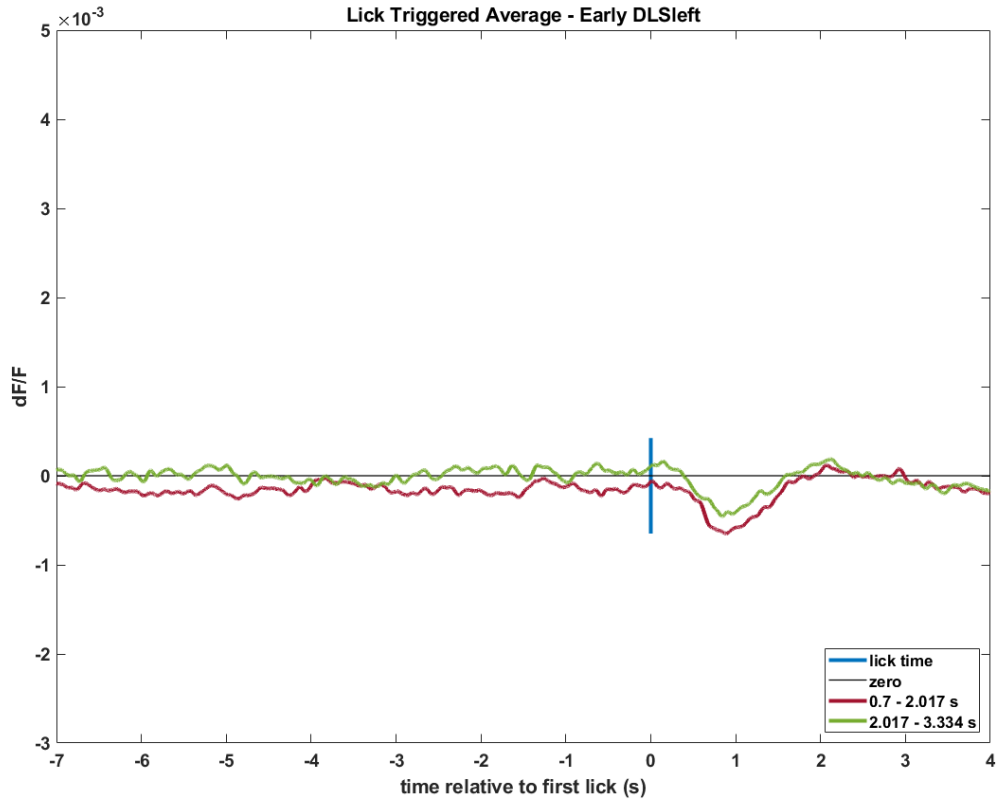

(a) *Mouse 4 - left side*

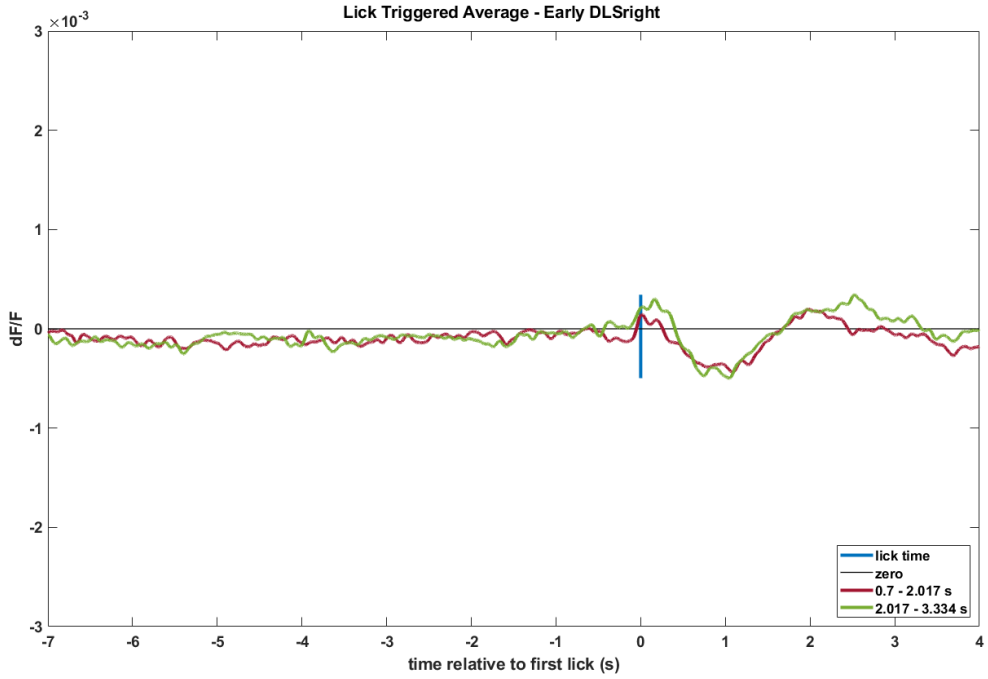

(b) *Mouse 4 - right side*

Figure 4.12: dF/F signal form fiber implanted in the right and left dorsolateral striatum for 2075 early trials in mouse 4.

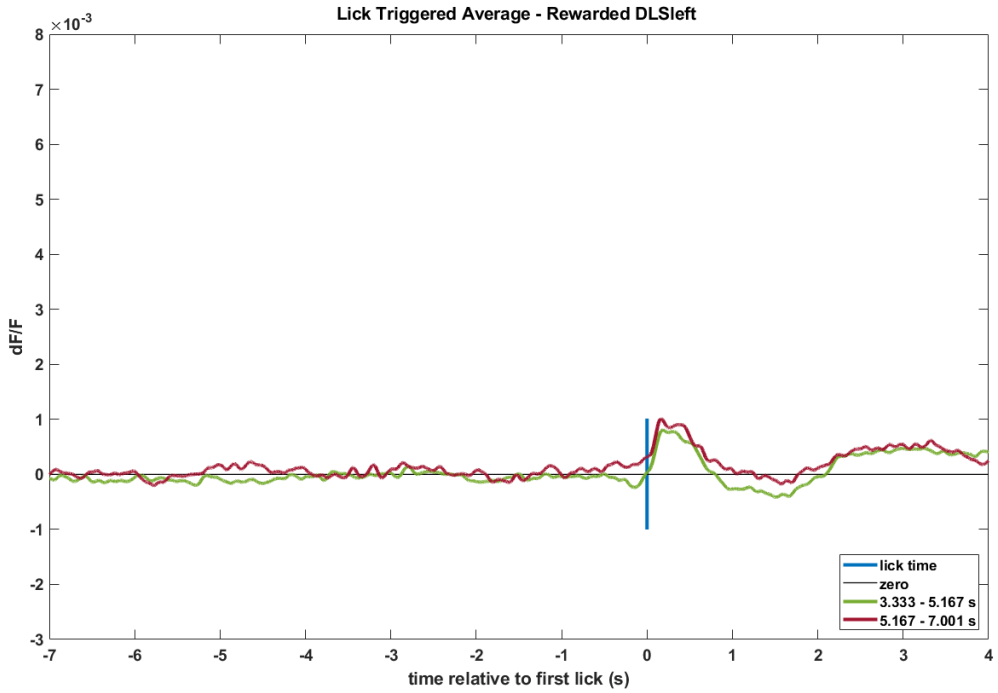

(a) *Mouse 4 - left side*

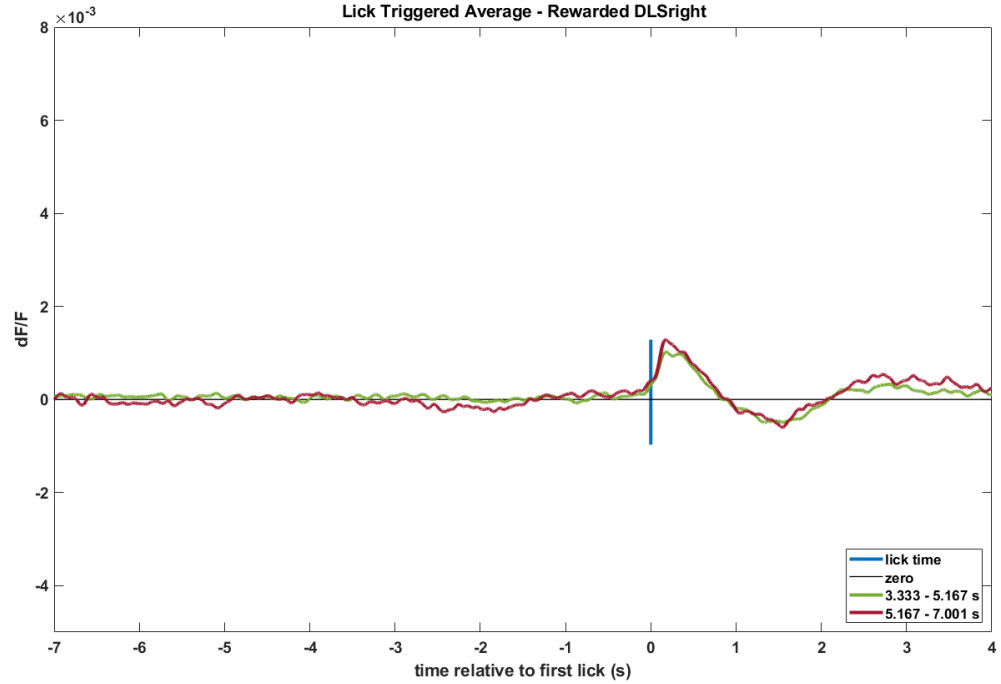

(b) *Mouse 4 - right side*

Figure 4.13: dF/F signal form fiber implanted in the right and left dorsolateral striatum for 1272 rewarded trials in mouse 4.

4.3 Artefacts

Motion artefacts must be taken into account when photometric signal is analyzed. They can derive from two different types of movements: known and unknown. Known movements are the ones that usually acquisition system can capture giving wrong information about the number of licks in the trials: every time the sensor detect a lick, it can be a real lick or simply the mouse that touches the tube by doing other movements, for example grooming. Sometimes mouse starts groom during a session tounching the tube with an high frequency. The trials in which the mouse grooms should be eliminated in order to lower the noise of signal. One way to recognize grooming is to watch the mouse during the recording session and keep note of trials involved. Grooming events have a distinguished pattern in the raster plot and so they can be recognized also looking at raster plot after the session instead of watching the mouse during the training/recording. An example of raster plot is shown in Figure 4.14. Each row is a trial, and per each trial licks (green dots) are represented in function of the time (ms). Vertical lines in the plot represent early and rewarded windows (blue and black lines), the cue time (light blue line) and the reaction window (pink line). Around trials number 792-793, 861-862, high frequency of licks represents the typical pattern of grooming behavior. In order to exclude grooming trials, the raster is observed for each day and they are manually excluded.

There are also unknown movements that may modulate the neuronal signal. During all the sessions, mice had accelerometer on their back; it allows to sense vibrations on the mouse measuring acceleration on the three axes. Output signal of the accelerometer (V) gives non-constant values if the mouse is moving during the acquisition. In this way, the xyz accelerometer values can reveal if there is a relationship between the behavior and magnitude of the activation in direct-pathway neurons. As Figure 4.15 shows, around the first lick time mouse doesn't move a lot.

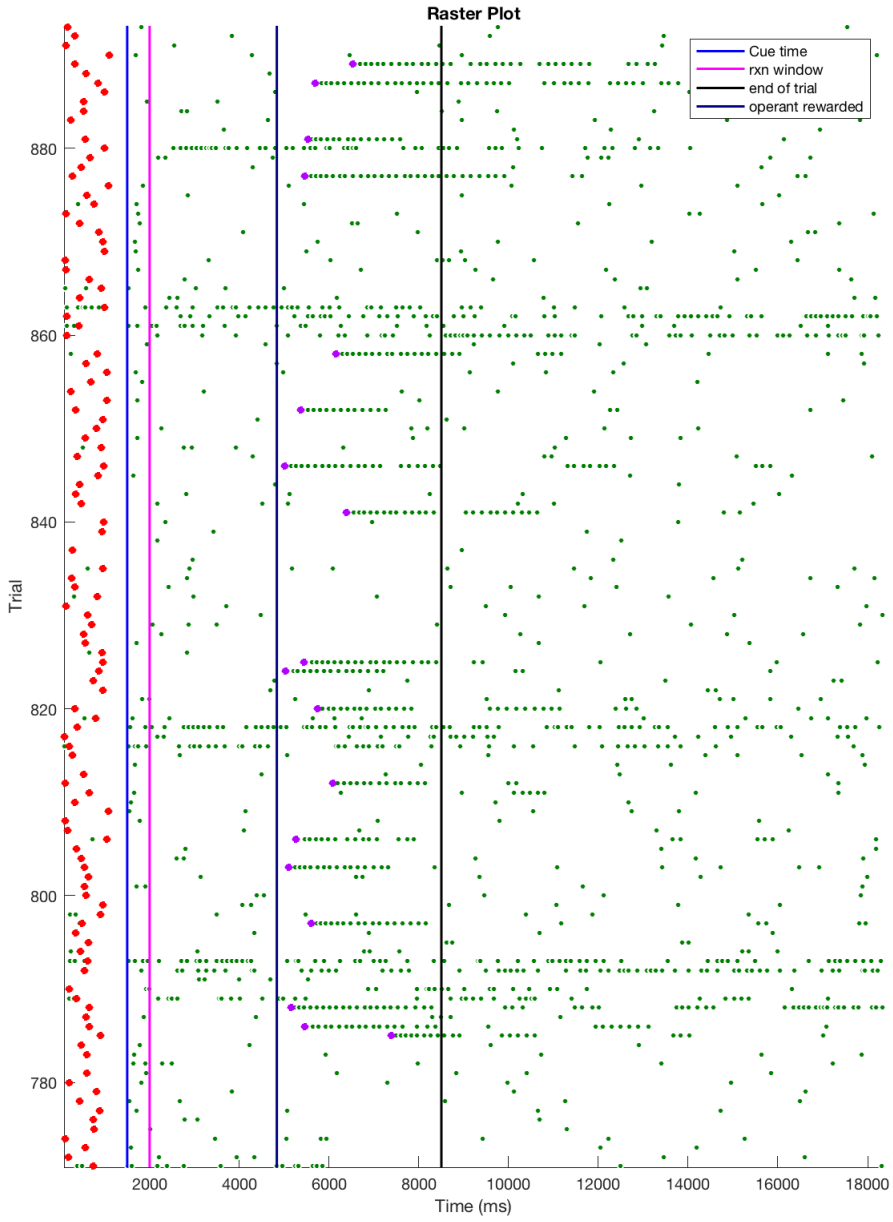

Figure 4.14: Raster Plot example

So it can be hypothesized ramps seen in the dF/F signal aren't associated with ongoing movements of the animal. In particular, in Figure 4.15, the one on the top shows dF/F signal for mouse 1 during one day of acquisition and the one on the bottom represents the signal for z-axis from the accelerometer over time relative to the first lick per each trial, early and rewarded. All the signals are aligned to the time of first lick (zero in the time-axis).

Also signal from x and y axes are shown in Figure 4.16. If the accelerometer is perfectly perpendicular to the ground (when positioned on the back of the mouse), x and y axes should not sense any acceleration. But, most of the time, also in this case there is information about the posture of the mouse. The amplitude of the position signal confirms that tha mouse was not moving significantly correspond to the ramps in neural activity.

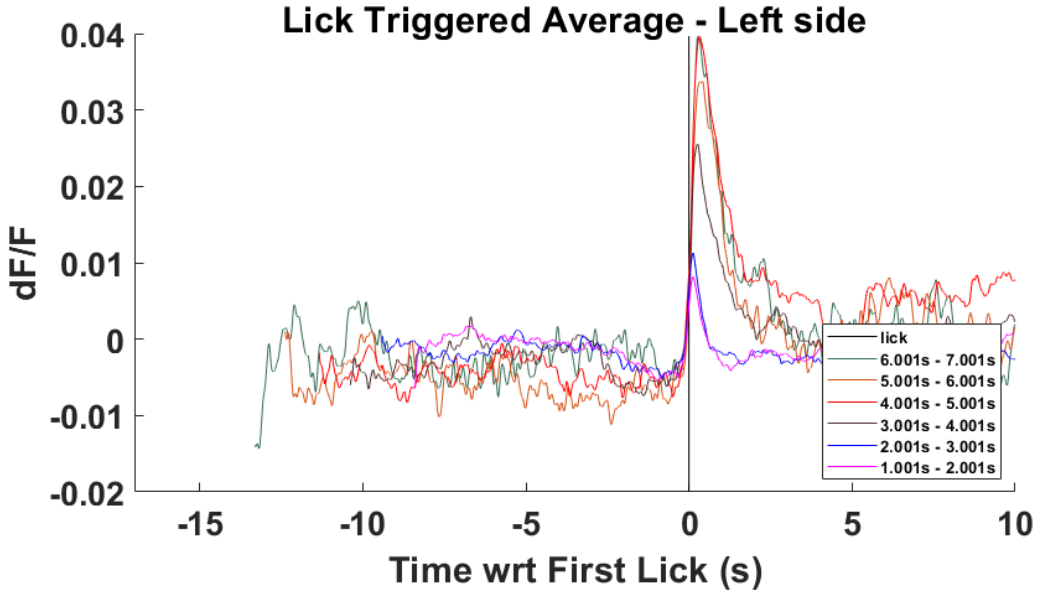

(a) *Mouse 1 - left side*

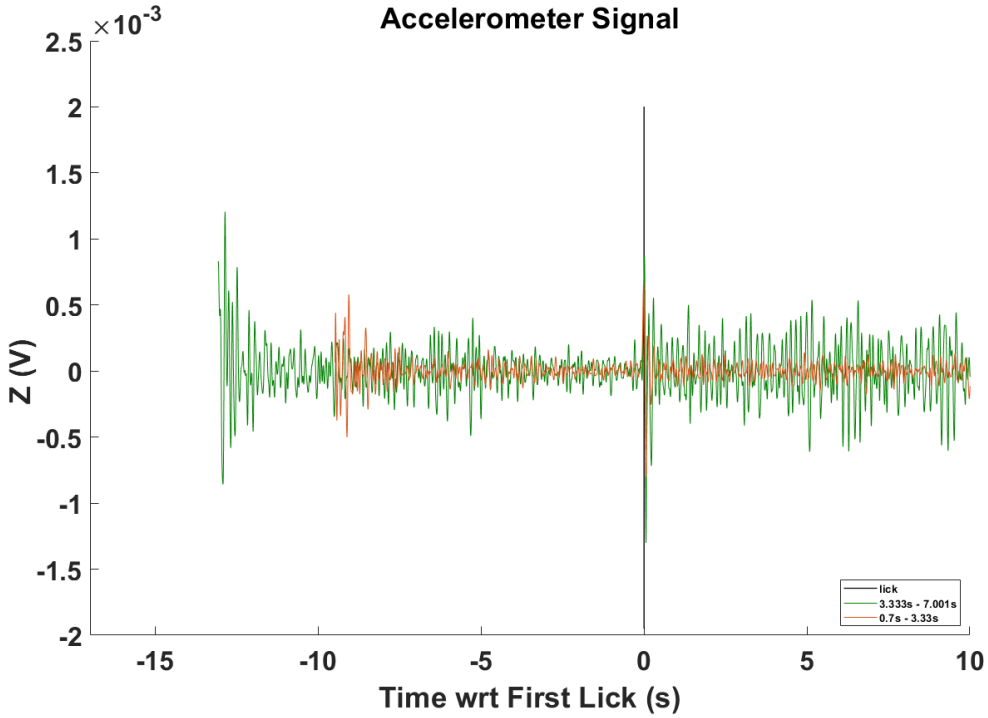

(b) *Accelerometer, z-axis*

Figure 4.15: dF/F signal and Accelerometer signal for z-axis.

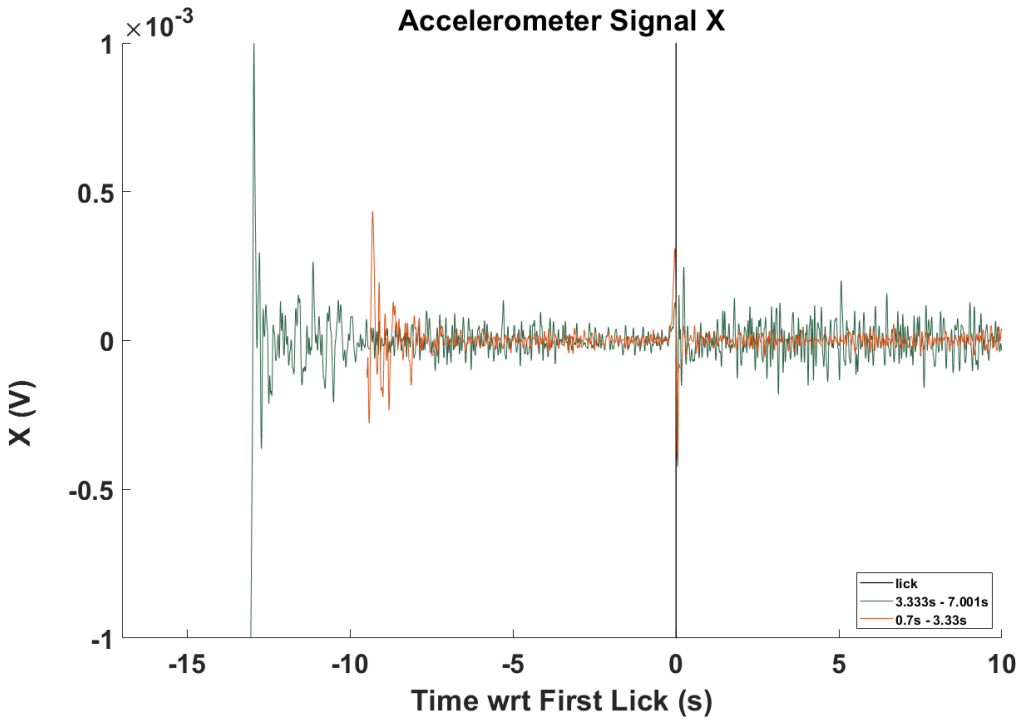

(a) *Acceloremeter, x-axis*

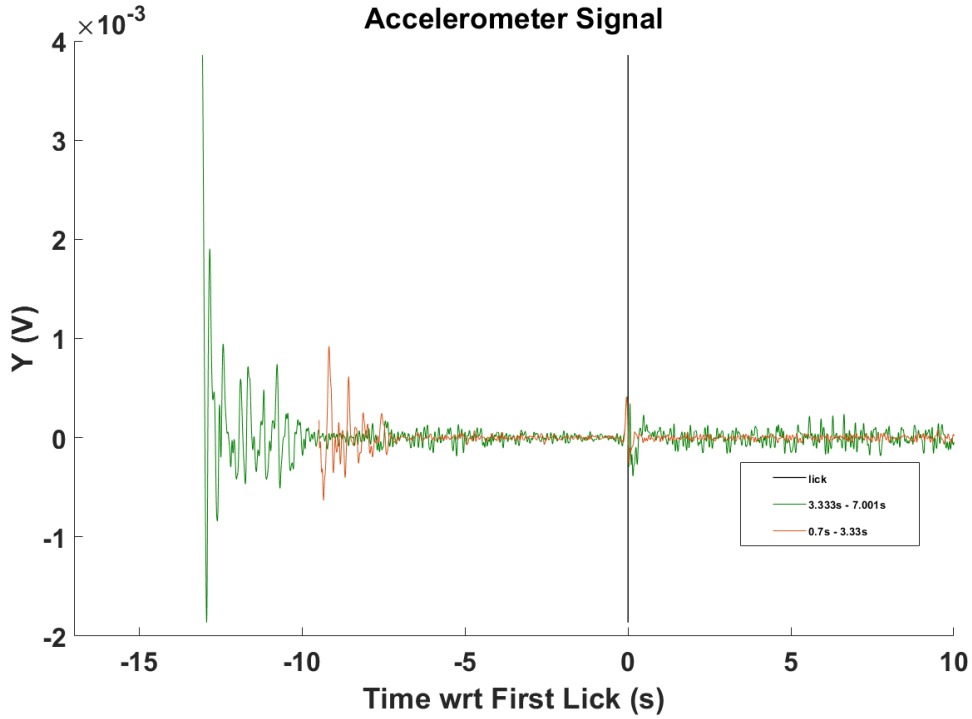

(b) *Accelerometer, y-axis*

Figure 4.16: Accelerometer signal for x and y axes.

Chapter 5

Conclusions and Future Improvements

The first experiment of this thesis project has been conducted implanting bilaterally two flat cut optical fibers into striatum of two mice and injecting AAV vectors containing GCaMP6f indicator to label D1-type neurons. Histological images of the mice's brain show the expression of the virus and the position of the fibers in the striatum. The dF/F, obtained from the fluorescence signal recorded from behaving mice, contains ramps supposed to be related to the movement timing. The signal has a similar trend and amplitudes in both mice. Mouse's position in the three axes (x-, y-, z-) reveals that ramps in activation of direct-pathway neurons are not related to physical movements of the animal. The experiment has been repeated using novel tapered optical fibers coated with silk solution. Changes in fluorescence obtained from signal recorded in three different mice contains only noise and not information about the calcium signal. Histological images obtained from one mouse confirm a very low expression of the fluorescent molecule in the striatum. Probabily, during the implant of the fibers, the polymer was not dry enough and, when the

devices were lowered in the brain, silk solution remained concentrated in the cortex. The poor expression of the GCaMP indicator in D1-type neurons didn't allow to use tapered optical fibers to analyze simultaneously neural activity at different depths in the striatum. For these reasons, the experiment could be performed again implanting the fibers coated with silk solution few days after the deposition of the polymer in order to be drier. Once the expression of the indicator is obtained in neurons of striatum, the neural activity at different level along the length of the tapered fiber may be compared illuminating small regions from localized sites using mirror to change input light angle.

Bibliography

[1] Matt Carter. *Guide to research techniques in neuroscience*. Academic Press, 2015.

[2] Cody A Siciliano and Kay M Tye. Leveraging calcium imaging to illuminate circuit dysfunction in addiction. *Alcohol*, 2018.

[3] Benjamin A Flusberg, Axel Nimmerjahn, Eric D Cocker, Eran A Mukamel, Robert PJ Barretto, Tony H Ko, Laurie D Burns, Juergen C Jung, and Mark J Schnitzer. High-speed, miniaturized fluorescence microscopy in freely moving mice. *Nature methods*, 5(11):935, 2008.

[4] Kasey S Girven and Dennis R Sparta. Probing deep brain circuitry: new advances in in vivo calcium measurement strategies. *ACS chemical neuroscience*, 8(2):243–251, 2017.

[5] Fritjof Helmchen, Michale S Fee, David W Tank, and Winfried Denk. A miniature head-mounted two-photon microscope: high-resolution brain imaging in freely moving animals. *Neuron*, 31(6):903–912, 2001.

[6] Guohong Cui, Sang Beom Jun, Xin Jin, Michael D Pham, Steven S Vogel, David M Lovinger, and Rui M Costa. Concurrent activation of striatal direct and indirect pathways during action initiation. *Nature*, 494(7436):238, 2013.

[7] Melissa R Warden, Jessica A Cardin, and Karl Deisseroth. Optical neural interfaces. *Annual review of biomedical engineering*, 16:103–129, 2014.

[8] Search kopf instruments model 1900 stereotaxic alignment system.

[9] Ferruccio Pisanello, Gil Mandelbaum, Marco Pisanello, Ian A Oldenburg, Leonardo Sileo, Jeffrey E Markowitz, Ralph E Peterson, Andrea Della Patria, Trevor M Haynes, Mohamed S Emara, et al. Dynamic illumination of spatially restricted or large brain volumes via a single tapered optical fiber. *Nature neuroscience*, 20(8):1180, 2017.

[10] Marco Pisanello, Andrea Della Patria, Leonardo Sileo, Bernardo L Sabatini, Massimo De Vittorio, and Ferruccio Pisanello. Modal demultiplexing properties of tapered and nanostructured optical fibers for in vivo optogenetic control of neural activity. *Biomedical optics express*, 6(10):4014–4026, 2015.

[11] Skyler L Jackman, Christopher H Chen, Selmaan N Chettih, Shay Q Neufeld, Iain R Drew, Chimuanya K Agba, Isabella Flaquer, Alexis N Stefano, Thomas J Kennedy, Justine E Belinsky, et al. Silk fibroin films facilitate single-step targeted expression of optogenetic proteins. *Cell reports*, 22(12):3351–3361, 2018.

[12] Neuronal electrophysiology: the study of excitable cells.

[13] Karel Svoboda and Ryohei Yasuda. Principles of two-photon excitation microscopy and its applications to neuroscience. *Neuron*, 50(6):823–839, 2006.

[14] Gcamp: Next-generation genetically encoded calcium indicators.

[15] George Paxinos, Charles Watson, Michael Pennisi, and Ann Topple. Bregma, lambda and the interaural midpoint in stereotaxic surgery with rats of different sex, strain and weight. *Journal of neuroscience methods*, 13(2):139–143, 1985.

[16] KB Franklin and George Paxinos. *The mouse brain in stereotaxic coordinates, compact. The coronal plates and diagrams*. Amsterdam: Elsevier Academic Press, 2008.

[17] Doric lenses. http://doriclenses.com/.

[18] Chengbo Meng, Jingheng Zhou, Amy Papaneri, Teja Peddada, Karen Xu, and Guohong Cui. Spectrally resolved fiber photometry for multi-component analysis of brain circuits. *Neuron*, 98(4):707–717, 2018.

[19] Cleave (fiber).

[20] Eleanor M Pritchard, Patrick B Dennis, Fiorenzo Omenetto, Rajesh R Naik, and David L Kaplan. Physical and chemical aspects of stabilization of compounds in silk. *Biopolymers*, 97(6):479–498, 2012.

[21] Andrew Wilz, Eleanor M Pritchard, Tianfu Li, Jing-Quan Lan, David L Kaplan, and Detlev Boison. Silk polymer-based adenosine release: therapeutic potential for epilepsy. *Biomaterials*, 29(26):3609–3616, 2008.

[22] Jozsef Csicsvari, Darrell A Henze, Brian Jamieson, Kenneth D Harris, Anton Sirota, Péter Barthó, Kensall D Wise, and GyoÌĺrgy BuzsaÌĄki. Massively parallel recording of unit and local field potentials with silicon-based electrodes. *Journal of neurophysiology*, 90(2):1314–1323, 2003.

[23] Kunal K Ghosh, Laurie D Burns, Eric D Cocker, Axel Nimmerjahn, Yaniv Ziv, Abbas El Gamal, and Mark J Schnitzer. Miniaturized integration of a fluorescence microscope. *Nature methods*, 8(10):871, 2011.

[24] György Buzsáki. Large-scale recording of neuronal ensembles. *Nature neuroscience*, 7(5):446, 2004.

[25] Tsai-Wen Chen, Trevor J Wardill, Yi Sun, Stefan R Pulver, Sabine L Renninger, Amy Baohan, Eric R Schreiter, Rex A Kerr, Michael B Orger, Vivek Jayaraman, et al. Ultrasensitive fluorescent proteins for imaging neuronal activity. *Nature*, 499(7458):295, 2013.

[26] Thetastation-1.

[27] Irwin H Lee and John A Assad. Putaminal activity for simple reactions or self-timed movements. *Journal of neurophysiology*, 89(5):2528–2537, 2003.